



PhD in Molecular Medicine XXIV Cycle
Molecular Oncology

***Characterization of CA IX interactome:
new insights on a highly versatile
carbonic anhydrase***

Tutor:

Prof. N. Zambrano

Internal Co-supervisor:

Prof. L. Del Vecchio

External Co-supervisor:

Prof. F. Maina

Coordinator:

Prof. F. Salvatore

PhD Student: Dr. Francesca Monteleone

Academic Year 2011-2012

*To the most important
person in my life,
my mother*

ABSTRACT	5
1. INTRODUCTION	7
1.1 Carbonic Anhydrases	7
1.1.1 CA IX	9
1.2 The Armadillo and HEAT repeats	20
1.3 The nucleocytoplasmic transport	23
1.3.1 Nuclear import	24
1.3.2 Nuclear export	26
1.3.3 Ran-dependent transport	26
1.4 The Ubiquitin-Proteasome Pathway	28
1.4.1 Ubiquitin Ligases (E3s)	30
1.4.2 CAND1	32
2. AIM OF THE PROJECT	37
3. RESULTS	38
3.1 CA IX expression in normoxic and hypoxic HEK-293 cells	38
3.2 CA IX interactome in normoxic and hypoxic HEK-293 cells	38
3.3 Validation of XPO1, TNPO1 and CAND1 as CA IX interactors	44
3.4 Identification of the minimal CA IX sequence required for the interaction with XPO1, TNPO1 and CAND1	46
3.5 Native complexes of XPO1 and CA IX in HEK-293 cells	46
3.6 Analysis of subcellular distribution of CA IX in normoxic and hypoxic HEK-293 cells	48
3.7 Identification and analysis of putative NES and NLS in CA IX sequence	50
3.8 Comparison of subcellular distribution of CA IX among different cell lines	57
3.9 In vivo expression and localization of CA IX	57
3.10 Functional validation of CA IX- CAND1 interaction	59
4. MATERIAL AND METHODS	61
4.1 Cell lines and experimental treatments	61
4.2 DNA constructs	61
4.3 Cell lysates preparation, interactome characterization and mass spectrometry protein identification	63
4.4 Bioinformatic analysis	64

4.5	<i>Antibodies, interaction assays and western blot analysis</i>	65
4.6	<i>Fluorescence and immunofluorescence analyses</i>	65
4.7	<i>Immunohistochemical analysis</i>	66
5.	DISCUSSION	67
6.	ACKNOWLEDGEMENTS	71
7.	REFERENCES	72

ABSTRACT

CA IX is a member of the carbonic anhydrase family of enzymes. It is a well known marker of hypoxia and is involved in pH regulation, migration/invasion and survival in hypoxic cancer cells. It is indicative of a poor prognosis in many cancer types and is associated with resistance to conventional therapy. So, there is a diffuse interest in inhibiting its function. Unfortunately, small molecule inhibitors that are available to inhibit CA IX demonstrated to be not much selective because of a high degree of homology amongst the catalytic sites of the various CA isoforms.

The main aim of my PhD project was to identify molecular interactors of CA IX, and through them, to contribute to clarification of CA IX biological mechanisms. These molecules may drive design and development of peptide mimetics interfering with CA IX function.

A complex protein network of novel CA IX interactors has been highlighted: several proteins belong to the family of the ARM and HEAT-repeat containing proteins and several members of the nucleocytoplasmic transport machinery have been identified as CA IX interactors under hypoxia, including importins and exportins. XPO1 and TNPO1 have been chosen as representative members of the nucleocytoplasmic transport machinery.

Cullin-associated NEDD8-dissociated protein 1 (CAND1) is a nuclear HEAT/ARM-containing protein that is involved in gene transcription and assembly of the SCF E3 ubiquitine ligase complex. It interacts with CA IX under both normoxic and hypoxic conditions.

Immunofluorescence (IF) analysis further proved complex subcellular localization of CA IX in human cell lines, highlighting a nuclear accumulation of CA IX in hypoxic cells. Nuclear presence of CA IX was also observed in two out of seven cases of clear cell renal cell carcinoma (ccRCC).

Putative NLS/NES sequences have been identified in CA IX protein sequence; IF analysis showed that they are able to affect distribution of reporter protein GFP inside the cell.

Collectively these data suggest that subcellular localization and functions of CA IX are more complex than previously thought. CA IX may have intracellular functions different from those already known at the plasma membrane. Investigation on this

emerging scenario may prove useful to highlight unsuspected features in CA IX biology and its involvement in molecular mechanisms of cancer.

1. INTRODUCTION

1.1 Carbonic Anhydrases

Carbonic Anhydrases (CAs; also known as Carbonate Dehydratases EC 4.2.1.1) are ubiquitous zinc metalloenzymes present in prokaryotes and eukaryotes that catalyze the reversible hydration reaction of carbon dioxide (CO_2) to bicarbonate (HCO_3^-) and protons (H^+). They are encoded by five evolutionarily unrelated gene families that are the α -CAs (present in vertebrates, bacteria, algae and cytoplasm of green plants); the β -CAs (predominantly in bacteria, algae and chloroplasts of monocotyledons and dicotyledons); the γ -CAs (mainly in archaea and some bacteria); the δ -CAs and ζ -CAs (present in some marine diatoms)¹⁻⁵.

In mammals, 16 α -CA isozymes or CA-related proteins with different catalytic activity, subcellular localization and tissue distribution are present⁶⁻¹³. In human they are fifteen, as the CA XV gene is expressed in rodents, but appears to have become a pseudogene in primates¹⁴. They can be classified according to various criteria including subcellular localization, catalytic activity and expression pattern. Accordingly, we can now describe intracellular (CA I-III, VA, VB, VII, VIII, X, XI, XIII) and extracellular (CA IV, VI, IX, XII, XIV), catalytically active (CA I-VII, IX, XII-XIV) and inactive (CA VIII, X, XI), wide-spread (CA II, IV, VB, XII, XIV) and restricted to few tissues (CA I, III, VA, VI, VII) carbonic anhydrases (**Figure 1**). Different combinations of the above listed properties create a series of features, allowing each isoform to fulfil a unique role in a specific physiological context¹⁵.

CAs are usually expressed in well differentiated metabolically active cells and tissues. Among all isoforms, CA II is the most widely distributed, being almost ubiquitous, and one of the most efficient catalyst¹⁶.

The CA reaction is involved in many physiological and pathological processes based on gas exchange, ion transport and pH balance, such as respiration and transport of CO_2 and bicarbonate between metabolizing tissues and lungs; pH and CO_2 homeostasis; electrolyte secretion in various tissues and organs; biosynthetic reactions (gluconeogenesis, lipogenesis and ureagenesis); bone resorption; calcification; production of body fluids; digestion; renal acidification and

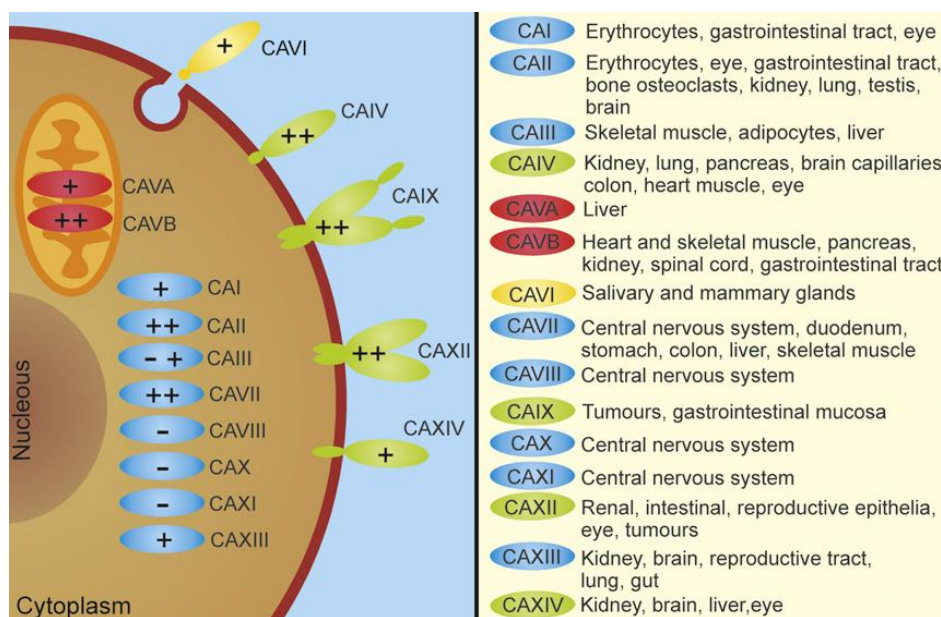


Figure 1. Schematic representation of 15 members of human α -Carbonic Anhydrase family. The intracellular CAs possess only the catalytic domain; the transmembrane CAs have a transmembrane region and also a cytoplasmic tail. Peculiar features are shown by the extracellular CAs, CA VI and CA IX, devoid of the intracellular tail or possessing unique N-terminal proteoglycan-like domain, respectively (Truppo et al.; *Bioorg. Med. Chem. Lett.* **2012**, 22, 1560–1564).

tumorigenicity⁶⁻⁹. As a consequence, many CAs are important therapeutic targets that may be inhibited to treat a range of disorders including edema, glaucoma, obesity, cancer, epilepsy and osteoporosis¹⁷.

Among all isoforms, CA IX is particularly interesting, as it is overexpressed in many cancer types and often associated to radio/chemo-resistance^{18, 19}.

1.1.1 CA IX

CA IX is a peculiar member of the CA family, because of both structural properties and subcellular distribution. Moreover, as CA XII¹⁸, it is a tumor-associated isoform and its expression is a negative prognostic factor²⁰⁻²³, also indicative of resistance to conventional therapy²⁴.

It was discovered in HeLa cells using monoclonal antibody M75 and initially termed MN⁶. MN consisted in a transmembrane glycoprotein, whose expression was regulated by cell density and correlated with tumorigenicity²⁵. It was also detected in clinical specimens of cervical and some others human carcinomas and was absent in normal tissues of corresponding organs²⁶.

The cDNA of CA IX was described by Pastorek et al. in 1994²⁷, as a cDNA coding for the novel human protein MN. Based on striking homology between the central part of the MN protein and carbonic anhydrases and on capability of binding zinc and catalyze CA reaction, MN was considered as a new α -carbonic anhydrase isozyme, that was designed as CA IX by Hewett-Emmett and Tashian in 1996²⁸.

The MN/CA IX protein consists of 459 amino acids that are organized in an N-terminal signal peptide (aa 1–37), an extracellular part (aa 38–414), a transmembrane region (aa 415–434), and an intracellular C-terminus (aa 435–459). The extracellular part is further composed of two distinct domains: the PG-like domain (53-111) and CA domain (135-391)²⁹.

Gene and transcriptional regulation

The MN/CA IX gene was characterized by Opavsky et al. in 1996; it consists of 11 exons and 10 introns and encompasses 10.9 Kb²⁹ in the p12-p13 region of the chromosome 9³⁰. The first exon encodes the putative signal peptide and the entire PG-like domain, the exons 2-8 encode the CA domain and finally the exons 10 and

11 encode the transmembrane region and the intracellular tail, respectively²⁹ (**Figure 2**).

Even if the intron distribution in the CA domain coding region as well as the amino acid sequence homology suggest an early divergence in evolution of MN/CA IX gene, MN CA IX protein has highly conserved catalytic domain, indicating a functional importance of its catalytic activity²⁹.

The -173 to +31 fragment was identified as MN/CA IX promoter by deletion analysis. It contains six *cis*-acting elements: five regions protected in DNase I footprinting (PR1-PR5)³¹ and a HRE element **TACGTGCA**, corresponding to the -3/-10 sequence between the transcription start and PR1, that is activated by the hypoxia inducible-factor (HIF)³². Among them, five (HRE, PR1, PR2, PR3, PR5) positively affect and one (PR4) negatively affects CA IX transcription³¹. More specifically PR1 (-45/-24) and PR5 (-163/-145) bind Sp1/Sp3 factors³³⁻³⁵, PR2 (-71/-56) binds AP-1^{31, 35}, PR3 (-101/-85) binds proteins from nuclear extracts³¹ and finally repressor binding PR4 has not been identified.

The HRE is the most critical regulatory element in the CA IX promoter^{32, 34}; binding of HIF complex to HRE is a prerequisite for recruiting the transcriptional machinery to the CA IX promoter. So other regulatory elements act amplifying signals received at the HRE.

The minimal CA IX promoter also includes PR1 and, as said, is dependent on Sp1/Sp3 activity; Kaluz et al., have proposed that PR1 and HRE form a novel type of hypoxia-responsive enhancer element³⁴ (**Figure 3**).

CA IX transcription is highly inducible, but no mRNA is detected in the basal, uninduced state²⁷.

Hypoxia, through HIF-1, is directly involved in regulation of CA IX expression. This has been demonstrated both *in vivo* and *in vitro*; on one hand in tumor samples CA IX immunostaining is mostly restricted to hypoxic regions^{32, 36}, on other hand CA IX is expressed in most cancer cell lines only under hypoxic conditions^{32, 37}.

HIF-1 consists of two subunits: one is the oxygen-regulated HIF-1 α subunit, the other is the constitutively expressed HIF-1 β (also known as ARNT)³⁸. Under normoxic conditions, HIF-1 α is targeted for ubiquitin-mediated degradation by the 26S

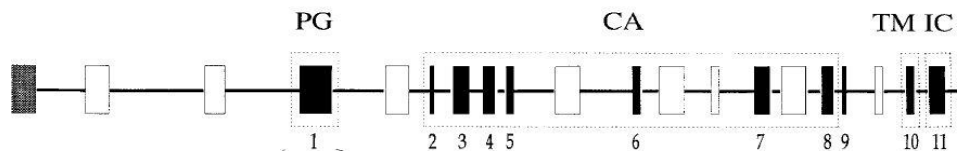


Figure 2. Map of human CA IX gene (Opavsky et al.; *Genomics* 1996, 33, 480-487).

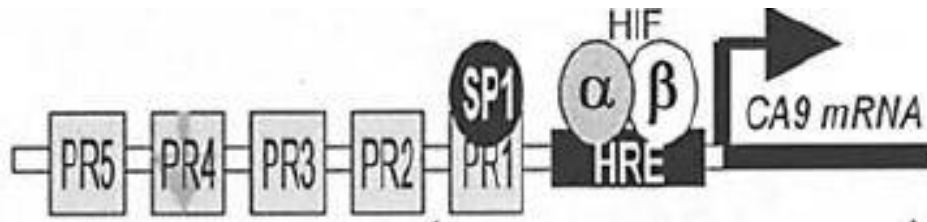


Figure 3. Schematic representation of -173/+31 promoter region of CA IX. The promoter of CA IX gene is formed by five protected regions (PR1-5) and a HRE element. The region PR1 together with HRE element constitute the minimal CA IX promoter and activate CA IX gene transcription through Sp1 and HIF respectively (Ihnatko et al; *International Journal of Oncology* 2006, 29, 1025-1033).

proteasome. This process is primarily regulated by prolyl hydroxylases (PHDs) which hydroxylate proline residues (Pro402 and Pro564 of HIF-1 α) localized within an oxygen-dependent degradation domain (ODDD). These allow binding of the VHL protein (pVHL), a component of the VCB E3 ubiquitin ligase complex^{39, 40}. Moreover, HIF-1 α is hydroxylated at asparagine residue (Asn803) within the C-terminal transactivation domain (C-TAD) by the factor inhibiting HIF-1 (FIH-1) which prevents binding of the p300/CBP coactivator^{41, 42}. Under hypoxic conditions, hydroxylation and acetylation are inhibited and therefore, pVHL cannot target HIF-1 α for degradation. After accumulation of HIF-1 α in the nucleus and dimerization with HIF-1 β , HIF-1 mediates essential homeostatic responses to cellular and systemic hypoxia by activating transcription of multiple genes (e.g. VEGF, Glut1, CA IX) whose promoters contain HREs (5'-RCGTG-3')⁴³ (**Figure 4**).

In addition to hypoxia, other agents and genetic factors can induce CA IX expression but majority of them converge on the HIF-1 pathway by regulating HIF-1 α stability, HIF-1 transcriptional activity or both⁴⁴. For example, inactivating mutations or epigenetic silencing of VHL associate to overexpression of CA IX under normoxic conditions through stabilization of HIF-1 α ^{32, 33, 45}; p53 activation is linked to CA IX down-regulation through increased proteasome-dependent degradation of HIF-1 α and by competing for CBP/p300^{46, 47}; high cell density, corresponding to mild hypoxia, causes CA IX overexpression through an increased PI3K activity, that in turn upregulates HIF-1 α levels or activity in a cell-type specific manner^{48, 49}. A further level of complexity in the understanding of CA IX transcriptional regulation is added by different kinetic of HIF-1 α and CA IX; the first is quickly degraded in normoxia and quickly stabilized in hypoxia, whereas CA IX is slowly both activated and degraded in hypoxia. This discrepancy may explain those cases in which CA IX expression does not correlate with hypoxic markers. So, HIF-1 α ⁺ CA IX⁻ cell profile may indicate that cells have recently become hypoxic and CA IX protein is not yet measurable. Conversely HIF-1 α ⁻ CA IX⁺ cell profile may indicate that cells had been hypoxic and have been reoxygenated but they still express long-lived CA IX⁴⁴. Finally it has to be taken into account that HIF-1 can be also regulated by O₂-independent factors, such as oncogenes and oncosuppressors⁵⁰, free radicals⁵¹.

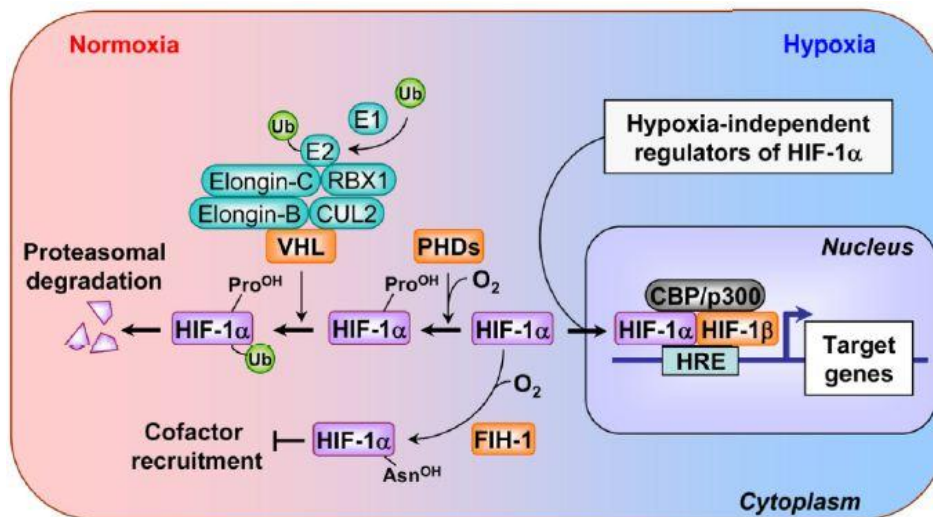


Figure 4. HIF-1 regulation pathway. In normoxia HIF-1 α protein is quickly degraded by 26S proteasome as polyubiquitylated by VHL, that recognizes and binds proline hydroxylated by PHDs. Moreover, asparagine hydroxylation by FIH-1 prevents CBP/p300 co-activator recruitment, so inhibiting transcriptional activity of HIF-1. In hypoxia both PHDs and FIH-1 are inhibited by lowered O₂ tension and HIF-1 α can translocate to the nucleus, where it associates to HIF-1 β , forming a complex that activates transcription of genes whose promoter contains HRE elements (Lu et al.; *Clin. Cancer Res.* 2010, 16, (24), 5928–5935).

CA IX gene is transcribed into a 1.5 Kb mRNA²⁷. So far, two splicing variants have been described: full length and AS. The first variant is predominant, low expressed in very few normal tissues and induced in hypoxic cancer cells; conversely, the second is less abundant in tumors, being not mainly dependent on hypoxia and cell density, but it can be detected in normal tissues and under normoxia. AS CA IX variant lacks exons 8 and 9 and produces a truncated form of CA IX protein, which is lacking the transmembrane region, intracellular tail and C-terminal part of the catalytic domain. Subsequently, it is incorrectly distributed; it is not localized at the plasma membrane, but mainly occupies intracellular space and is also released to the extracellular medium. Moreover, it is unable to form oligomers and shows reduced catalytic activity. It may behave in a dominant negative fashion, interfering with the function of the endogenous, hypoxia-induced FL protein⁵² (**Figure 5**).

Protein structure and function

At the beginning, structure of CA IX protein was analysed on the basis of sequence homology with other family members²⁷, then it was studied through x-ray crystallography⁵³. As already introduced, CA IX is described as a transmembrane, multi-domain glycoprotein consisting of a N-terminal proteoglycan (PG)-like region, a carbonic anhydrase (CA) catalytic domain, a transmembrane (TM) segment, and an intracellular (IC) tail^{27, 29}. Biochemical characterization of CA IX demonstrated that it forms dimers through a symmetrical intermolecular disulfide bond involving C137 localized on the backbone of the catalytic domain⁵⁴. Moreover, CA IX contains an intramolecular disulfide bond (C119–C299), a unique N-linked glycosylation site at Asn 309, in the catalytic domain, which is modified by high mannose-type glycans, and an O-linked glycosylation site at Thr 78, next to the PG domain. The recently reported crystal structure of the CA domain of this enzyme confirmed its dimeric nature and showed that the N-terminal regions of both monomers are located on the same face of the dimer, whereas the C-terminal ones are situated on the opposite face (**Figure 6**).

The CA IX catalytic domain appeared as a compact globular domain; the active site is located in a large conical cavity in the bottom of which the zinc ion is buried. The catalytic site is delimited by two distinct regions made of hydrophobic (Leu91, Val121, Val131, Leu135, Leu141, Val143, Leu198 and Pro202) or hydrophilic amino

A

```

hCA IX      MAPLCPSFWLPLLI FAPAPGLTVQLLSLLLLMPVHFQRLFRMQEDSFLGGGSSGGEDDPL
AS-hCAIX    MAPLCPSFWLPLLI FAPAPGLTVQLLSLLLLMPVHFQRLFRMQEDSFLGGGSSGGEDDPL

hCA IX      GEEDLPSEEDSFPREDPPGEEDLPGEEDLPGEEDLPEVKPKSEEEGSLKLEDLFTVEAPG
AS-hCAIX    GEEDLPSEEDSFPREDPPGEEDLPGEEDLPGEEDLPEVKPKSEEEGSLKLEDLFTVEAPG

hCA IX      DPQEPQNNAHREKEGDDQSHWRYGDDPPWFRVSPACAGRFQSFVDIRFQLAAFPALRPL
AS-hCAIX    DPQEPQNNAHREKEGDDQSHWRYGDDPPWFRVSPACAGRFQSFVDIRFQLAAFPALRPL

hCA IX      ELLGFQLPPLPELRIRNNGHSVQLTLPFQLEMALGFGREYRALQIILWGAGRPGSSIT
AS-hCAIX    ELLGFQLPPLPELRIRNNGHSVQLTLPFQLEMALGFGREYRALQIILWGAGRPGSSIT

hCA IX      VEGHRFPAEIHVVHILSTAFARVDEALGRPGGLAVLAAFLAEEGPEENSAYEQLLSRLEETA
AS-hCAIX    VEGHRFPAEIHVVHILSTAFARVDEALGRPGGLAVLAAFLAEEGPEENSAYEQLLSRLEETA

hCA IX      EESSETQVFGLDISALLP3DFSRVFQYEGSLITPPCAGGV IWTVFNQIVMLSAKQLHTLS
AS-hCAIX    EESSETQVFGLDISALLP3DFSRVFQYEGSLITPPCAGGV IWTVFNQIVMLSAKQVTS--

hCA IX      DTLNGPGDSRLQLNERATQPLNGRVIEASEFAGVDS5FRAAEPVQLNSLAAGIILALVY
AS-hCAIX    -----

hCA IX      ILLFAVTSVAFILVSMRQRHRRGTGGVSYRPAEVAETGA
AS-hCAIX    -----

```

B

Figure 5. Human splicing variants of CA IX. (A) Match between amino acid sequences deduced from the human FL and AS CA IX cDNA. AS hCA IX lacks the C-terminal part of the catalytic domain (grey background), the transmembrane region (black background) and the intracellular tail. Dashes correspond to residues deleted in AS-hCA IX (B) Schematic representation of the human FL and AS CA IX proteins (Barathova et al.; *British Journal of Cancer* **2008**, 98, (1), 129 – 136).

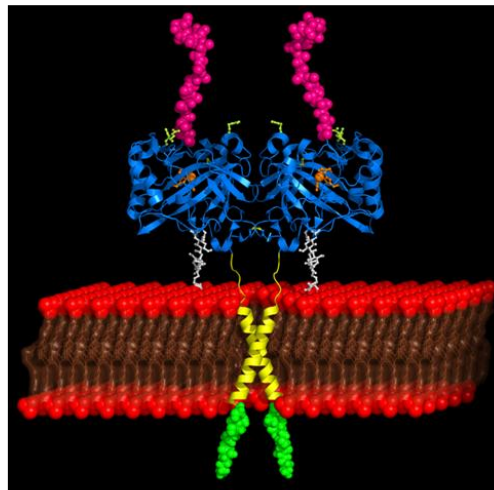
A**B**

Figure 6. CA IX structure and domain organization (A) CA IX dimer structure on the cell membrane, based on the X-ray crystallography data. The PG-like domain (53-111) is reported in magenta, the catalytic domain (135-391) in cyan, the transmembrane region (415-433) in yellow and finally the intracellular tail (434-459) in green (Alterio et al.; *PNAS* **2009**, 106, 38, 16233–16238); (B) Schematic representation of domain organization of CA IX highlighting its main biochemical features. C137 mediates CA IX dimerization, whereas C119 and C299 form an intramolecular disulfide bond. T78 and N309 are sites of O- and N- glycosylation respectively (Swietach et al.; *Oncogene* **2010**, 29, 6509–6521).

acids (Arg58, Arg60, Asn62, His64, Ser65, Gln67, Thr69, and Gln92) and spans from the surface to the center of the protein⁵³.

Each domain of CA IX protein has been associated to specific functions⁵⁵.

The PG-like domain, a region of around 60 amino acids that is a distinctive feature of CA IX, is involved in cell-cell adhesion, intercellular communication⁵⁶⁻⁵⁸ and, most probably, also in tumor invasion through interaction with β -catenin^{55, 58, 59}. Moreover it seems to contribute to the improvement of the CA IX catalytic activity at the acidic pH values at which it generally operates, especially in the hypoxic cells⁵³. Otherwise CA reaction would be highly disadvantaged at acidic pH values, as optimal pH for CO₂ hydration would be around neutral values. Presence of PG-like domain confers to CA IX an optimal activity at pH 6.49 differently to all other isoforms that work better in the pH range 6.9-7.1⁶⁰.

In 2003 Zavada et al. demonstrated that the whole extracellular domain (ECD) of CA IX can be released into the cell culture medium or into the body fluids of tumor patients⁶¹; this process is metalloprotease-mediated and is regulated by TACE/ADAM 17 but its biological function is unknown. CA IX ECD represents 10% of total CA IX under both normoxia and hypoxia; it may affect full length CA IX functions interacting with its binding partners⁶².

The CA domain has been associated to the growth and survival of tumor cells⁵⁵ and recently also to an increase of cell migration⁶³.

Finally, the intracellular tail (IC) was seen to be essential for correct functioning of CA IX, because its removal changes CA IX subcellular localization, whereas its mutagenization reduces ectodomain shedding and cell dissociation capacity of CA IX and abolishes the capability to acidify extracellular medium under hypoxia⁶⁴. Previously, it has been related to signal transduction through phosphorylation of a Tyr residue that allows interaction with regulatory subunit of PI3K and subsequent activation of Akt and other cancer-related signaling pathways⁶⁵.

Recently, our investigations have highlighted presence of putative nuclear localization sequences (NLS) and nuclear export sequences (NES) in the intracellular tail and transmembrane region respectively, that seem to drive intracellular distribution of CA IX⁶⁵.

CA IX expression is slowly activated but, once CA IX is present, it is very stable with a half-life of 2-3 days^{67, 68}. It is evident up to 96 hours after re-oxygenation and its

expression level reduces very slowly⁶⁷⁻⁶⁹. Conversely, HIF-1 α is an indicator of oxygenation state, as it is quickly stabilized under hypoxic conditions and quickly degraded under re-oxygenation⁷⁰. Consequently CA IX expression does not always correlate with HIF-1 α stabilization, as seen in perinecrotic regions of solid tumors⁷¹.

Role in cancer disease

CA IX is a tumor-associated enzyme. According to its involvement in tumorigenesis, CA IX is normally present in only few normal tissues, such as the gastrointestinal tract, whereas it is highly expressed in the perinecrotic hypoxic regions²⁴ of many cancer types including gliomas/ependymomas³, mesotheliomas³, papillary/follicular carcinomas³, carcinomas of the bladder⁷², uterine cervix^{73, 74}, nasopharyngeal carcinoma⁷⁵, head and neck⁷⁶, breast^{21, 24, 77}, oesophagus³, lungs²², brain³, vulva³, squamous/basal cell carcinomas³, and kidney⁷⁸ tumors. Differently in renal cell carcinoma CA IX is expressed also under normoxic conditions in the presence of VHL inactivating mutations that stabilize HIF-1 α ⁷⁹⁻⁸².

Strong tumor-association of CA IX mainly arises from almost exclusive transcriptional activation of the CA IX gene by HIF-1 α , that is the master regulator of cellular response to hypoxic stress³².

CA IX is a well established endogenous marker of hypoxia^{67, 83, 84}. Hypoxia is a key event in tumor progression deriving from excessive tumor growth rate, that exceeds the capacity of the host vasculature, with subsequent inadequate blood supply. It is a feature of many solid tumors and correlates with their aggressiveness and resistance to anti-cancer therapies. Indeed, hypoxia triggers architectural and phenotypic rearrangements of tumor tissue, resulting in the development of necrotic areas surrounded by zones of surviving hypoxic cells, that often become the most aggressive tumor cells⁸⁵.

Cancer cells respond to hypoxic stress mainly through stabilization and activation of HIF-1 α that in turn triggers expression of genes encoding for proteins involved in glucose metabolism, blood vessel growth, oxygen carriage, iron metabolism, cell migration and pH control. As a consequence of hypoxic conditions cancer cells undergo an adaptative glycolytic switch that leads them to become mainly dependent on glycolysis rather than on oxidative phosphorylation for energy production. Anaerobic metabolism is maintained also after re-oxygenation, as it produces

metabolic intermediates, namely pyruvate and lactate, that can be used for the biosynthesis of amino acids, nucleotides, and lipids, all important to sustain high cell proliferation rate of tumor cells⁸⁶. Use of anaerobic glycolysis by cancer cells also under normoxic conditions has been described as the “Warburg effect”^{87, 88}.

To survive cancer cells have to maintain a physiological intracellular pH (pH_i) value; one consequence of hypoxia-mediated acidosis is exactly the alteration of the intracellular pH, a decrease in which rapidly affects basic cellular functions, including membrane integrity, metabolism and energy production and proliferation^{86, 89}. So they have to release in extracellular space the pyruvate and lactate produced through anaerobic glycolysis, creating a pH gradient characterized by acidic pH values around 6 in the extracellular microenvironment, in contrast to normal tissues, which has characteristic pH values around 7.4, and by slightly alkaline pH values within them, which are optimal for their proliferation and survival⁹⁰.

As suggested by its orientation, CA IX function in hypoxic cancer cells consists in maintaining this pH gradient through acidification of extracellular pH (pH_e) and alkalization of intracellular one, so counteracting hypoxia-induced acidosis⁹¹. Indeed bicarbonate and protons produced by CA reaction contribute to further increase intracellular pH (pH_i) and decrease extracellular one, respectively⁹⁰. More specifically, CA IX interacts with bicarbonate transporters forming metabolon that allows bicarbonate to be transported back into the tumor cells where it contributes to maintain an intracellular pH (pH_i) value suitable for biosynthetic reactions^{55, 89}; alternatively bicarbonate can be transported to blood capillaries through anionic exchanger $\text{HCO}_3^-/\text{Cl}^-$. Moreover bicarbonate is a substrate for cell growth, as it is required in the synthesis of pyrimidine nucleotides^{3, 92}. Protons, however, remain in extracellular space, where they contribute to acidify extracellular pH. So, tumor cells decrease their extracellular pH (pH_e) both by excessive production of lactic acid and by CO_2 hydration catalyzed by CA IX^{90, 91, 93-98} (**Figure 7**).

Acidic extracellular pH (pH_e) confers a selective advantage to survival of cancer cells. Indeed, via promotion of chromosomal rearrangements, extracellular matrix breakdown, migration and invasion, induction of the expression of cell growth factors and protease activation, impairment of immune functions and finally protonation of weakly basic anticancer drugs, such as anthracyclines, that become impermeant, so reducing their uptake^{3, 92, 94, 96-102}.

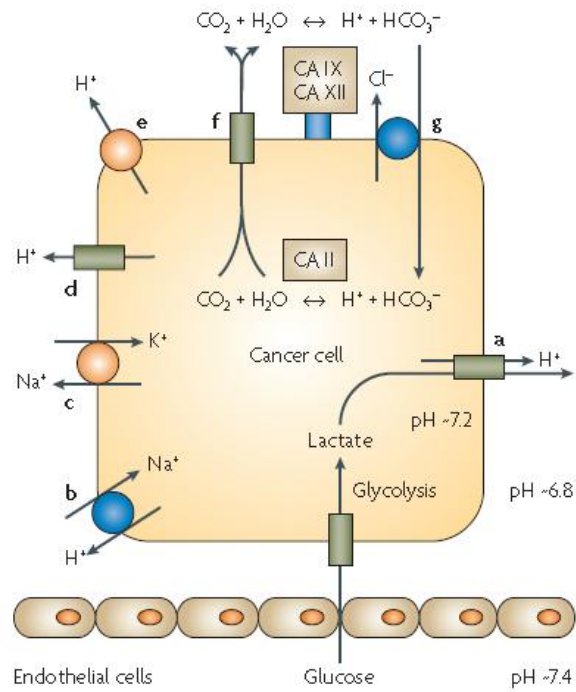


Figure 7. pH regulation within cancer cells. Cancer cells show a pH gradient characterized by acidic pH values in the extracellular microenvironment and by slightly alkaline pH values within them. To survive and better proliferate they maintain this gradient also through membrane-bound CAs, such as CA IX and CA XII, that catalyze hydration reaction of CO_2 to bicarbonate and protons. Bicarbonate comes back into the cell buffering intracellular pH, whereas protons accumulate in the extracellular microenvironment further acidifying it (Supuran; *Nat Rev Drug Discov* **2008**, 7, (2), 168-81).

As already introduced, CA IX is involved in tumorigenesis also through its capacity to modulate cell adhesion⁵⁸. So, it is not only a marker of tumor hypoxia, but it is functionally involved in pathogenesis of cancer disease.

Differential expression between normal and cancer tissues and membrane localization make CA IX protein a useful therapeutic target against cancer⁹². Several monoclonal antibodies and small molecule inhibitors are in various stage of clinical development^{58, 103}. Among inhibitors, two main classes are known: the metal-complexing anions and the unsubstituted sulphonamides and their bioisosteres, sulphamates and sulphamides.

A crucial problem in CAIs design is related to the high number of isoforms, their diffuse localization in many tissues and organs and the lack of isozyme selectivity of the presently available inhibitors¹. Among possible approaches to overcome this problem there are the addition of charged species, bulky entities such as FITC or albumin or hydrophilic sugar moieties limiting transport across the plasma membrane^{1, 9, 10, 86, 104}, bioreductive prodrugs that are activated by hypoxia^{12, 13}. In 2010 Cianchi et al., tested three CA IX inhibitors and showed they decrease cell proliferation and induce apoptosis through intracellular acidification that activates ceramide-controlled signaling pathways¹⁰⁵.

Strong dependence of CA IX expression from HIF-1 α and so hypoxia can be also exploited to synthesize some CA IX targeted fluorescent imaging agents employing sulphonamide targeting groups and NIR fluorochromes to develop a non-invasive approach to detect and to quantify CA IX in tumors and so, to measure tumor oxygenation both in pre-clinical research and in patients¹⁰⁶.

1.2 The Armadillo and HEAT repeats

Protein repeats vary from short amino acid repetitions to large repetitions containing multiple domains. They arise via intragenic duplication and recombination events and, whether advantageous, are fixed among populations. Their most common function deals with protein-protein interactions. They are more common in eukaryotic organisms than in prokaryotes^{107, 108}.

Two of such protein repeats are the Armadillo and HEAT repeats, that are α -helical domains of around 50 residues, which pack together to form elongated super-helices

or “solenoids”^{109, 110}. They are involved in many different cellular processes to which both take part mediating protein interactions¹¹¹.

The Armadillo (ARM) repeats derive their name from the product of the *D. melanogaster* segment polarity gene Armadillo, in which they were first found¹¹²; then they were also discovered in the junctional plaque protein plakoglobin¹¹³, in the tumor suppressor adenomatous polyposis coli (APC)¹¹⁴, and in the nucleocytoplasmic transport factor importin α ¹¹⁵.

They are highly conserved and, in the canonical form, consist of three helices: H1, that is the shorter, H2 and H3 that are the longer. The H2 and H3 helices pack against each other in an antiparallel fashion and are roughly perpendicular to the shorter H1 helix, with a sharp bend between helices H1 and H2 mediated by a conserved glycine residue¹¹⁶.

The HEAT repeats are so named from four diverse eukaryotic proteins in which they were first identified: Huntingtin, Elongation factor 3, PR65/A subunit of protein phosphatase A and TOR¹¹⁶. They are also present in importins β 1 and β 2, in proteins related to the clathrin-associated adaptor complex¹¹⁶, in the microtubule-binding colonic and hepatic tumor-related protein (CTOG) family¹¹⁷ and in many others proteins related to chromosome dynamics¹¹⁸.

The typical HEAT repeats consist of a pair of anti-parallel helices, A and B, which form a helical hairpin. The repeats are usually stacked in parallel, so that the A and B helices of each repeat are parallel to the corresponding helices in an adjacent repeat, creating a double layer structure in which the A and B helices form the outer convex and inner concave faces, respectively¹⁰⁹. Being variable in length, amino acid sequence and 3-D structure HEAT repeats have been divided in three classes; AAA, IMB and ADB¹¹¹.

Even if the ARM and HEAT repeats are differently organized, their structure and function are very similar, with helices H1 and H2 corresponding to strongly bent helix A and helix H3 corresponding to helix B¹¹¹. Often these latter helices of each repeat form the groove in which protein interactions occur¹⁰⁷ (**Figure 8**).

A common phylogenetic origin but a divergent evolution has been suggested for the ARM and HEAT repeats¹¹⁹⁻¹²¹. To confirm this suggestions these latter share seven

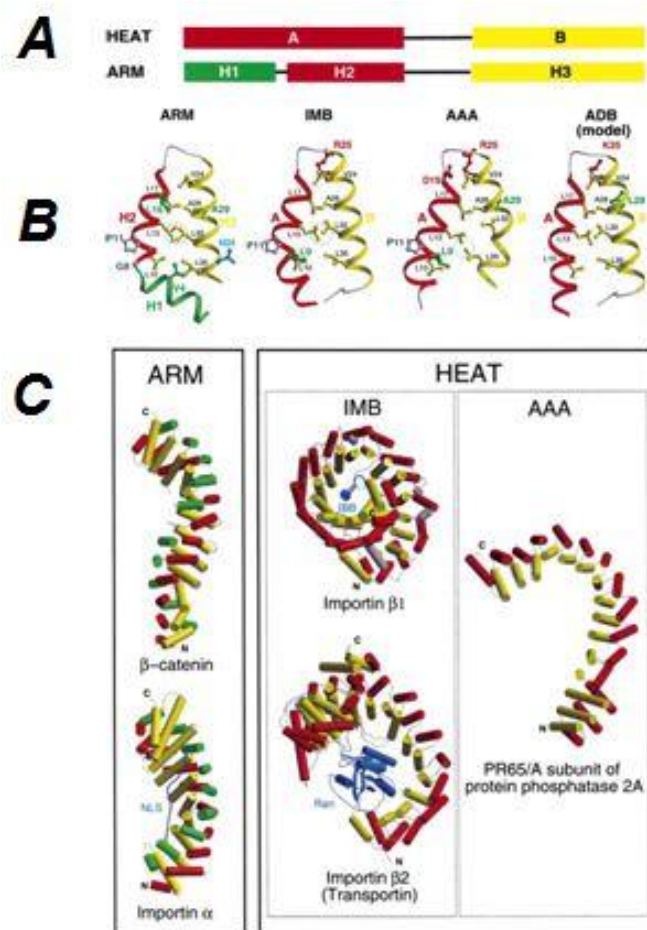


Figure 8. The ARM and HEAT repeats. (A) Schematic representation of the ARM and HEAT repeat. Helix A of the HEAT repeat corresponds to helices H1 and H2 of the ARM repeat and helix B corresponds to helix H3 (B) Structural organization of specific ARM and HEAT repeats from importin α , importin β and the PR65/A subunit of phosphatase 2A (C) Some examples of ARM and HEAT repeat containing proteins Helix B/H3 of every repeat form the groove in which protein interactions occur. Ligand are in blue (Andrade et al.; *J. Mol. Biol.* **2001**, 309, 1±18).

highly conserved hydrophobic residues, located at positions 10, 13, 17, 24, 28, 32, and 35, that form the hydrophobic core of the repeat¹¹¹.

1.3 The nucleocytoplasmic transport

In eukaryotic cells the genetic material is enclosed in the nucleus; so proteins involved in replication and transcription of DNA, that occur in the nucleus, and mRNA molecules that are translated in the cytoplasm have to be exported from, or imported in the nucleus, respectively. This continuous movement of macromolecules occurs through the nuclear pore complex (NPC) that spans the nuclear envelope.

The NPC structure is highly conserved and each NPC consists of three main substructures: the cytoplasmic filaments, a central core and the nuclear basket. The central core connects cytoplasmic ring to nuclear one through eight spokes forming an aqueous channel. Each NPC results from assembly of about thirty different nucleoporins proteins; each protein is present in multiple copies^{122, 123}.

Nucleoporins are differently involved in the nucleocytoplasmic transport: transmembrane nucleoporins fasten the NPC to the nuclear envelope; FG-nucleoporins have FG-repeats, that represent sites of binding to karyopherins crossing the NPC.

B-karyopherins constitute a protein family of nucleocytoplasmic transport factors that includes at least 20 members in human. They are relatively large proteins of about 100 kDa and notoriously contain 19 to 20 HEAT repeats, so showing a superhelical structure that confers them an inherent flexibility that is important for conformational change associated with cargo binding¹²⁴. Their interaction with cargoes is regulated by RanGTP. B-karyopherins are distinguished in importins and exportins on the basis of specific transport that they mediate. They carry across the nucleus large dimension molecules that are unable to cross passively, by diffusion, the nuclear envelope. Indeed, the NPCs are impermeable to most macromolecules, with the exceptions of B-karyopherins, alone or associated to their cargo, as NPC recognition occurs at sites on the karyopherins distinct from those involved in cargo binding¹²⁵.

1.3.1 Nuclear import

Importins bind their cargo in the cytoplasm; interaction with it can be direct or mediated by an adaptor protein. The complex, once recognized by the NPC, is translocated to the opposite side of the nuclear envelope, where the cargo is released after association with RanGTP.

Importin β , also known as karyopherin β 1, mediates the nuclear import of proteins carrying the classical **N**uclear **L**ocalization **S**equences (NLS). It does not directly interact with them but via the adaptor protein importin α , that possessing at the N-terminus an importin β -binding domain (IBB) plus an NLS-binding domain, in turn recognize and binds the NLS.

Importin α , also known as karyopherin α , is an ARM repeat containing protein; its NLS-binding domain consists of 10 ARM repeats and interaction with cargo occur at the inner concave surface.

There are two types of NLSs: monopartite, such as the SV40 large T-antigen NLS (PKKKRKV¹²⁶), or bipartite, as the nucleoplasmin NLS (KR-10aa-KKKL¹²⁷)¹²⁸⁻¹³¹. The first consists of a cluster of three or five positively charged residues, the second has a further cluster of basic residues, that is separated from the monopartite-like structure by a linker of 10 to 12 residues.

In the nucleus RanGTP binds the complex importin β - importin α - cargo causing release of cargo. One possible mechanism is that RanGTP leads to dissociation of importin β from the complex importin β - importin α - cargo, subsequently causing destabilization of importin α - cargo bond.

Importin β can also directly interact with cargo containing classical NLSs. In this case, release of cargo in the nucleus is determined by mutually exclusive binding of cargo and RanGTP, as their binding site, at the N-terminal arch of importin β , are almost completely overlapping¹²⁶.

After release of cargo, importin α -RanGTP complex comes back to the cytoplasm associated with the exportin CAS (**Figure 9**).

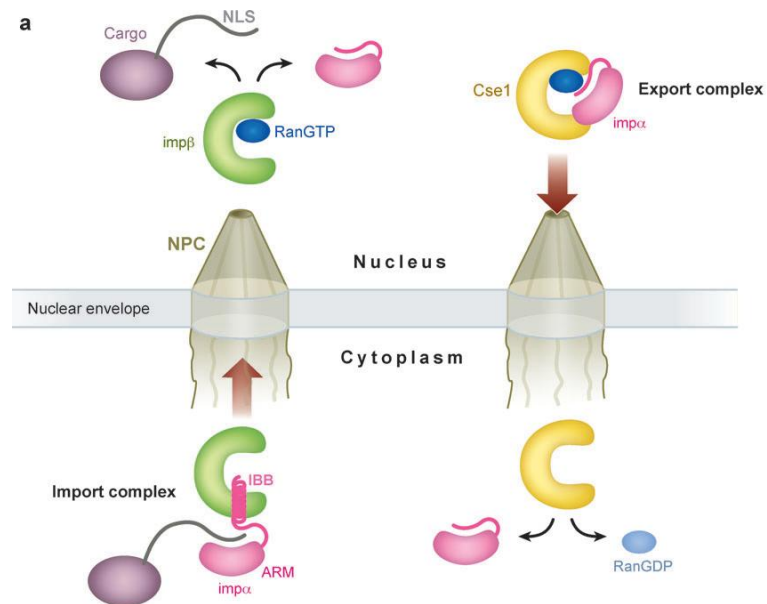


Figure 9. Schematic description of nuclear import. The NLS sequence present in the cargo to be imported is recognized by the adaptor molecule importin α ($\text{imp}\alpha$) via its armadillo-repeat domain (ARM). The importin β -binding (IBB) domain of importin α binds in a helical conformation to importin β ($\text{imp}\beta$). The cargo: $\text{imp}\alpha$: $\text{imp}\beta$ complex is transported to the nucleus via the nuclear pore complex (NPC), where it is dissociated upon the formation of importin β : RanGTP complex. In the absence of $\text{imp}\beta$, the IBB domain of $\text{imp}\alpha$ is autoinhibitory because it binds at the NLS-binding site. The adaptor $\text{imp}\alpha$ is recycled back by the exportin Cse1/CAS (Cook et al.; *Annu. Rev. Biochem.* **2007**, 76, 647–71).

1.3.2 Nuclear export

Conversely, exportins bind their cargo in the nucleus, in the presence of RanGTP. In the cytoplasm the cargo is released after hydrolysis of RanGTP to RanGDP.

The exportin Crm1, also known as exportin-1, mediates the nuclear export of cargoes containing the **N**uclear **E**xport **S**equence (NES) that is a hydrophobic leucine-rich sequence, such as the protein kinase A inhibitor (PKI) NES¹³² (**Figure 10**).

Leptomycin B is a small molecule that inhibits nuclear export mediated by Crm-1 through its covalent attachment to a cysteine residue of Crm-1, that interferes with cargo binding^{133, 134}.

Not only proteins are exported from the nucleus, also several types of RNA are transported in the cytoplasm¹³⁵. Exportin-t is involved in the transport of tRNA and exportin-5 in the transport of tRNA and microRNA precursors. In this last case the RNA hairpin structure with a 3' overhang is recognized as the NES^{136, 137}.

1.3.3 Ran-dependent transport

Ran is a small GTPase of 24 kDa belonging to the Ras superfamily. It is present as RanGTP in the nucleus and as RanGDP in the cytoplasm^{138, 139}. Hydrolysis of RanGTP to RanGDP is catalyzed by the RanGTPase-activating protein RanGAP, that is located in the cytoplasm and in turn is stimulated by the proteins RanBP1 and RanBP2^{140, 141}. RanBP1 is a 23-kDa cytoplasmic protein that contains a single Ran-binding domain (RanBD)¹⁴², whereas RanBP2 is a component of the cytoplasmic fibrils of the NPC and contains four RanBDs¹⁴³. The C-terminal domain of RanGAP is modified through covalent linkage to the ubiquitin-like protein SUMO-1 that localizes Ran-GAP to the cytoplasmic face of the NPC through interaction with RanBP2^{144, 145}.

After hydrolysis RanGDP comes back to the nucleus by the transport factor NTF2^{146, 147}, that specifically recognizes Ran in its GDP-bound state¹⁴⁹⁻¹⁵⁴. In the nucleus RanGDP is quickly re-converted to RanGTP by the guanine nucleotide exchange factor RanGEF, that is there located because of a interaction with chromatin through histones H2A and H2B¹⁵⁵ (**Figure 11**).

RanBP3 is another regulatory protein located in the nucleus that stimulates RanGEF activity¹⁵⁶.

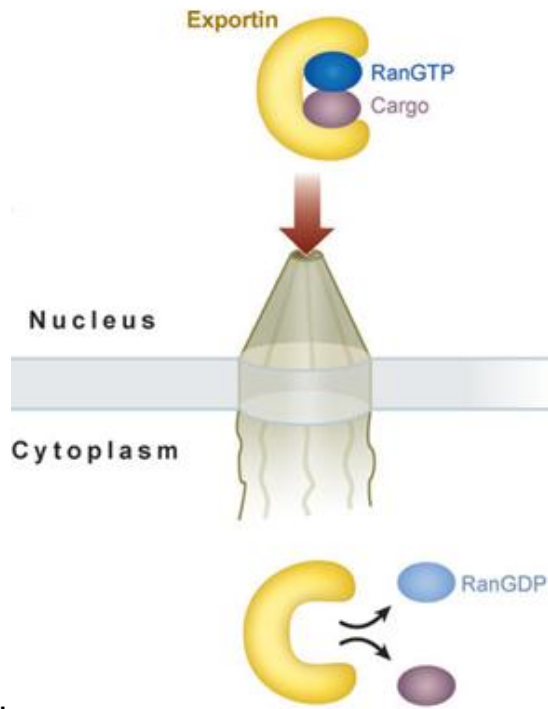


Figure 10. Schematic description of nuclear export. The NES present in the cargo to be exported in the cytoplasm is recognized by the nucleocytoplasmic transport factor Crm1 in the presence of RanGTP. In the cytoplasm cargo is released after hydrolysis of RanGTP to RanGDP (Cook et al.; *Annu. Rev. Biochem.* **2007**, 76, 647–71).

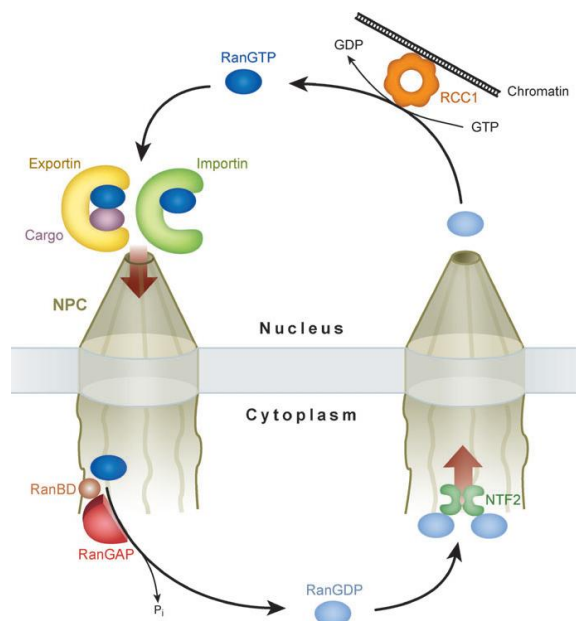


Figure 11. Schematic illustration of the Ran cycle. The high concentration of RanGDP in the cytosol is maintained by RanGAP, which is bound to the cytoplasmic fibrils of the nuclear pore complex. It acts on the RanGTP that enters the cytoplasm (via binding to exportins and importins). The high concentration of RanGTP in the nucleus is maintained by RanGEF, a chromatin-bound guanine exchange factor, which acts on the RanGDP, that enters the nucleus with its dedicated transport factor nuclear transport factor 2 (NTF2) (Cook et al.; *Annu. Rev. Biochem.* **2007**, 76, 647–71).

RanGAP localization in the cytoplasm and RanGEF localization in the nucleus allow to create a gradient of Ran GTP that ensures the directionality of the nucleocytoplasmic transport¹³².

1.4 The Ubiquitin-Proteasome Pathway

The Ubiquitin-Proteasome Pathway (UPP) is a system by which proteins are first targeted for degradation through ubiquitylation and then degraded through the 26S proteasome¹⁵⁷⁻¹⁵⁹.

Ubiquitylation is a post-translational modification which leads to formation of a covalent binding between ubiquitin, a small 76 amino acid protein, and a substrate protein. It is a complex three-step reaction which requires the sequential action of three enzymes: an ubiquitin-activating enzyme E1, an ubiquitin-conjugating or ubiquitin-carrier enzyme E2 and an ubiquitin-ligase E3.

In the first step E1 activates the C-terminal Gly residue (G76) of ubiquitin for nucleophilic attack through an ATP-dependent reaction that consists of an intermediate formation of ubiquitin adenylate, with the release of PPi, followed by the binding of ubiquitin to a Cys residue of E1 in a thiol ester linkage, with the release of AMP. In the second step activated ubiquitin is transiently transferred to an active site Cys residue of E2 through formation of a thioester bond. In the third and last step C-terminus of previously activated ubiquitin is linked to a ϵ -amino group of Lys residues of substrate protein forming an isopeptide bond^{160, 161}.

Ubiquitylation may be highly variable in length and linkage type. Substrates can be monoubiquitylated, via the attachment of a single ubiquitin, or multiubiquitylated, such that more than one amino acid is modified with monoubiquitin, or polyubiquitylated, such that ubiquitin is added sequentially to substrates to form ubiquitin chains¹⁶². In this last case the whole process of ubiquitylation usually consist of many cycles of the three-step reaction, in order to form the polyubiquitin chain, in which the C-terminus of each ubiquitin unit is linked to a specific Lys residue (most commonly Lys48) of the previous ubiquitin.

Indeed the address of polyubiquitylated substrates is indicated by which lysine within ubiquitin is linked to the C-terminus of an adjacent ubiquitin¹⁶³. The K48-linked

polyubiquitin chain serves as signal for proteosomal degradation¹⁵⁹, whereas the K63-linked polyubiquitin chain functions in signal transduction and DNA repair^{164, 165}.

Polyubiquitinated proteins are usually degraded by the 26 proteasome complex through an ATP-dependent reaction that produces different types of products: free peptides, short peptides still ubiquitylated and polyubiquitin chains. These last two products are converted to free and reusable ubiquitin by the action of ubiquitin-C-terminal hydrolases or isopeptidases¹⁵⁷.

The 26S proteasome is assembled in an ATP-dependent manner and consists of a catalytic component, the 20S proteasome and of a regulatory component, the 19S cap, that contains several ATPase subunits and other subunit involved in the action of the 26 proteasome on ubiquitylated proteins. Moreover, it mediates substrate recognition through interaction with polyubiquitylated chains¹⁵⁷.

Indeed, ubiquitin-binding proteins containing ubiquitin-binding domain (UBDs) are responsible for recognizing the different ubiquitin signals and targeting modified proteins to specific cellular processes, including ubiquitin/26S proteasome-mediated proteolysis¹⁶⁶. The predominant ubiquitin signal for UPP appears to be the K48-linked ubiquitin chain with a minimum length of four ubiquitin units¹⁶⁷. Specifically polyubiquitylated substrates to be degraded by the 26S proteasome are recognized by two types of ubiquitin receptors: those intrinsic 26S proteasome base subunits, such as Rpn10¹⁶⁸ and Rpn13^{169, 170}, which are capable of directly recognizing ubiquitylated substrates, and the ubiquitin-like domain (UBL)-containing shuttle factors, such as Rad23, Dsk2 and Ddi1, capable of targeting ubiquitylated substrates to the 26S proteasome, by binding ubiquitylated substrates and the 26S proteasome simultaneously using one N-terminal UBL and one to two C-terminal ubiquitin-associated (UBA) domains, respectively¹⁷¹⁻¹⁷⁴.

Before being degraded by the proteasome, substrates are deubiquitylated and unfolded to reach the catalytic center of the proteasome. Rpn13 contains a domain through which it binds and activates the deubiquitylating enzyme (DUB) Uch37¹⁷⁵⁻¹⁷⁷, so it might carry out a dual function¹⁷⁸.

1.4.1 Ubiquitin Ligases (E3)

Among enzymes involved in ubiquitylation reaction, E3 is that responsible mainly for the selectivity of ubiquitin-protein ligation as it binds specific protein substrates containing specific ubiquitylation signals.

There are multiple families of E3s or E3 multiprotein complexes that differ not only for substrate specificity, but also for action mechanism.

To date around a thousand of E3s have been identified and they have been divided into two main large groups:

- HECT domain E3s
- RING E3s

The **HECT domain family** comprises modular E3 enzymes with a highly variable N-terminus, interacting with a specific substrate, and an HECT domain, mediating E2 binding and the chemistry of ubiquitylation. More specifically, the latter consists in a region of about 350 amino acids containing a highly conserved cysteine residue, that acts as a site of thiolester formation with ubiquitin in an intermediary ubiquitin transfer reaction¹⁷⁹.

The **RING finger family** comprises single-subunit and multisubunit E3 enzymes¹⁸⁰⁻¹⁸³. The feature of these enzymes is that of showing in their sequence a series of histidine and cysteine residues with a characteristic spacing that allows for the coordination of two zinc ions in a cross-brace structure called the **Really Interesting New Gene** finger. E3s belonging to this family seem to function as molecular scaffolds. Similarly, to members of the HECT domain family, they also have a modular organization with the RING finger and regions near it involved in E2-dependent ubiquitylation of the substrate and the other domains recognizing substrate ubiquitylation signals.

Differently from HECT domain E3s, RING E3s catalyze direct transfer of the activated ubiquitin from E2 to the E3-bound substrate (**Figure 12**).

Among multisubunit RING E3s so far known, the SCF (Skp1-Cullin-F-box protein) E3 ubiquitin ligase complex has been well characterized. It catalyzes ubiquitylation of many important regulatory proteins taking part to diverse cellular pathway¹⁸¹. Among them there are Cdk inhibitor p27^{184, 185}, Cdk2 regulatory subunit cyclin¹⁸⁶⁻¹⁸⁸, NF-κB inhibitor IκB, and Wnt signal transducer β-catenin¹⁸⁹⁻¹⁹². Substrates such as the

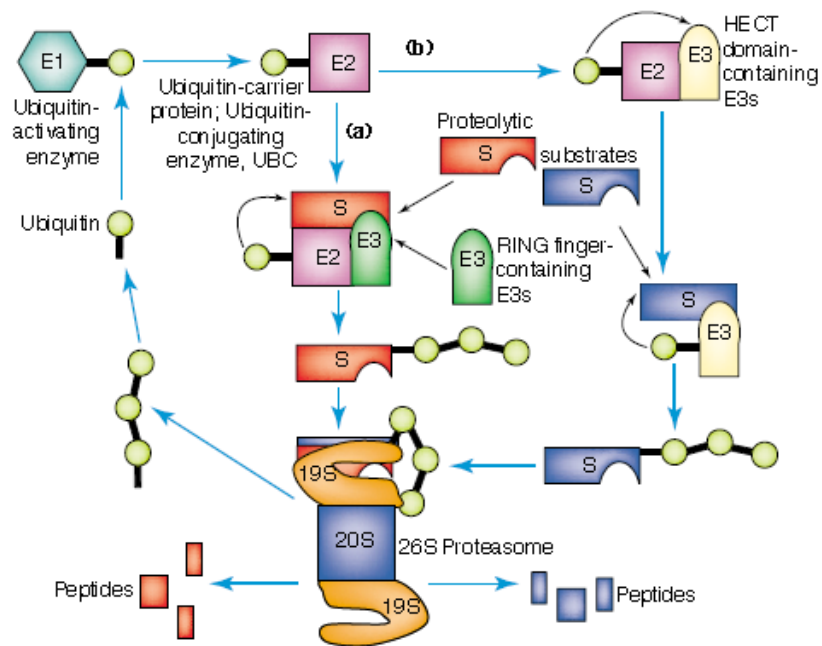


Figure 12. The Ubiquitin-Proteasome Pathway. Ubiquitin is first activated to a high-energy intermediate by E1. It is then transferred to a member of the E2 family of enzymes. From E2 it can be transferred directly to the substrate, when the E3 belongs to the RING finger family of ligases, or transferred first to the E3 before it is conjugated to the E3-bound substrate, when the E3 belongs to the HECT-domain-containing family of ligases. Multiple cycles of the basic three-step reaction allow to generate a polyubiquitin chain. The polyubiquitylated substrate so binds to the 26S proteasome complex (Ciechanover et al.; *Trends in Cell Biology* **2004**, 14, (3), 103-106).

cyclin E and the CDK inhibitor p27 are targeted to SCF complex by phosphorylation¹⁹³⁻¹⁹⁷, that seems to be the predominant signal. However, core oligosaccharides that have a high mannose content are also recognized by SCF in humans¹⁹⁸.

Within this complex the RING finger protein is Roc1; as already introduced, it has a molecular scaffold function^{199, 200} and strongly interacts with cullin. Moreover, it is involved in recruitment of E2²⁰⁰⁻²⁰³. Cul1 and Roc1 represent the catalytic core of the complex. Also Skp1 takes part to SCF complex; it functions as an adaptor protein that recruits the substrate-specific F-box proteins, which recognize the substrate F-box motif^{180, 204, 205}. Cul1/Roc1/Skp1/E2 represents a common platform to which the various F-box proteins competitively associate. All F-box proteins share the N-terminal region, that mediates their binding with Skp1, whereas differ at the C-terminal region, that is the protein-protein interaction domain and is involved in binding of substrate to be ubiquitylated. The E3 activity of the SCF complex is regulated through the ubiquitin-like protein Nedd8/Rub1, that is linked to a cullin specific lysine residue¹⁸⁰, located at the very C-terminal highly conserved winged – helix B (WH-B) domain^{206, 207}, by the Nedd8 E1, Nedd8 E2 and Roc1²⁰⁸⁻²¹² (**Figure 13**). SCF complex neddylation seems to be required for subsequent substrate polyubiquitylation^{210, 213, 214} and is a reversible reaction; Nedd8 removal from cullin is mediated by the eight subunit COP9 signalosome complex (CSN)²¹⁵. CSN has a metalloprotease activity based on the JAMM motif of the CSN5 subunit²¹⁶ and is present in eukaryotic cells; it binds SCF complex and remove Nedd8 by deneddylation. Additionally CSN recruits the deubiquitylating enzyme UBP12, which counteract the intrinsic ubiquitin-polymerizing activity of the catalytic core²¹⁷. Nevertheless, CNS is considered a positive regulator of SCF as it seems to protect F-box proteins from autocatalytic degradation in absence of substrates. In the presence of substrate deneddylation is inhibited²¹⁸.

Recent identification of an inhibitor of SCF complex, namely CAND1/TIP120A, has added new insights about regulation of assembly and disassembly of the SCF complex and role of neddylation cycle in these processes.

1.4.2 CAND1

The CAND1 protein was first found by Yogosawa et al in 1996 in rat liver nuclear extracts, using histidine-tagged TBP as a ligand for affinity-purification of proteins

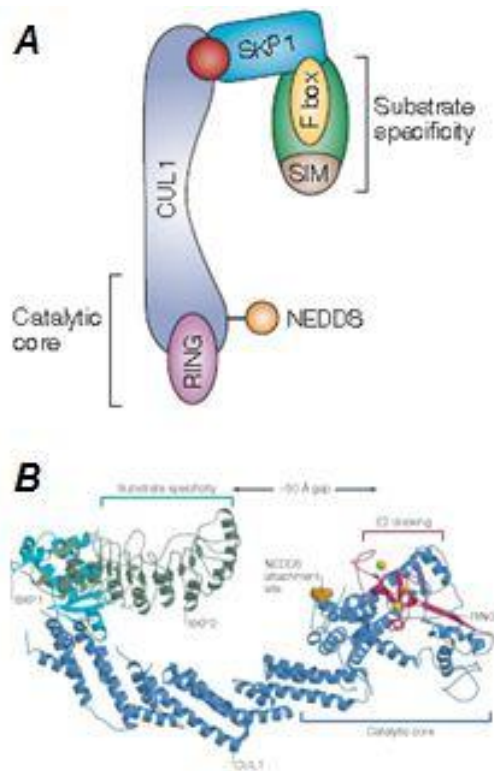


Figure 13. The SCF E3 ubiquitin ligase complex. (A) Schematic representation of SCF E3 complex. Roc1 (the RING protein) and Cul1 constitute the catalytic core of the complex. Cul1 has an elongated shape, with the RING protein bound to the C-terminal cullin-homology domain, near to a conserved Lys residue that is conjugated to Nedd8. The RING subunit is thought to function as the docking site for ubiquitin conjugating enzymes (E2s). Substrates are recruited through the adaptor protein SKP1 and an F-box-protein substrate receptor. (B) The crystal structure of the SCF^{Skp2} complex. The substrate-specificity module of SCF is separated from the E2-docking site by a series of three cullin repeats that form the curved N-terminal stalk of cullin-1 (Cul1) (Petroski et al.; *Nature Reviews Molecular Cell Biology* 2005, 6, 9-20).

bound to TBP; so, being a 120-kDa protein, it was named TBP-interacting protein 120 (TIP120)²¹⁹.

Cloning and characterization of TIP120/CAND1 cDNA allowed to find that it encoded for a novel polypeptide of 1230 amino acids²¹⁹.

Subsequent studies performed by Makino et al in 1999 showed the TIP120/CAND1 was able to activate basal transcription in vitro, in a dose-dependent manner, through the stimulation of recruitment of TFIIF/RNAPII into a pre-initiation complex²²⁰. Despite TIP120/CAND1 did not show any typical motifs that were often found in transcription factors, two regions, namely that acidic at the N-Terminus (202-370) and that comprising the two leucine-rich domains at the C-terminus (988-1230), that could function as transcription factor were identified. Indeed they were able to bind TBP and stimulate a basal transcription, so suggesting that TIP120/CAND1 could be a bipartite transcription factor²²¹.

The human gene of CAND1 is located in the q14 region of the chromosome 12. Four splicing variants have been identified that are correctly translated. TIP120A mRNA was seen to be highly expressed in the heart and in the liver, mildly expressed in the skeletal muscle and in the brain and low expressed in the spleen and in the lung²²². Conversely TIP120B (CAND2) that is 60% homologous to CAND1 is highly expressed in the skeletal muscle²²⁰.

As many nuclear proteins, CAND1 consists of 27 tandem HEAT repeats and shows as a nearly all-helical solenoid protein. Collectively these repeats form an unusually tertiary structure with the N-terminal half of CAND1 forming a right-handed superhelix and the C-terminal half forming a left-handed superhelix. The whole structure of CAND1 can be divided into three arches (N-terminal, C-terminal and central) that enclose the space involved in protein-protein interactions with cullins (**Figure 14**). CAND1 competes with Skp1 for binding to Cul1, around which coils, making multiple and extensive intermolecular contacts. Indeed, through an unusual B-hairpin CAND1 occupies part of the Skp1 binding site on Cul1, so blocking further assembly of the SCF complex. CAND1 only binds to Cul1 molecules that are not conjugated to Nedd8 because of steric hindrance that inhibit it²²³ (**Figure 15**).

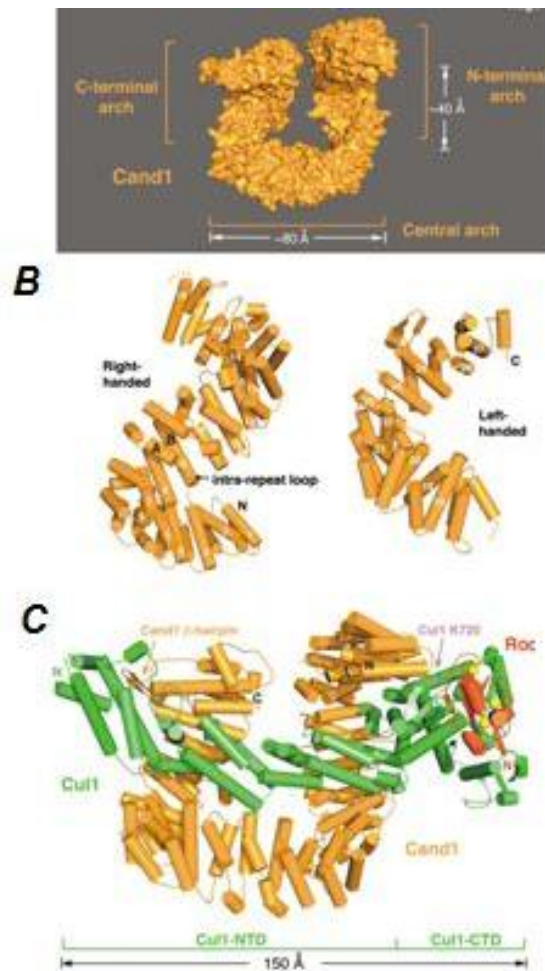


Figure 14. CAND1 structure. (A) Surface representation of CAND1 protein. In evidence three arches in which its overall shape can be divided (B) Opposite handedness of N- and C-terminus of CAND1 (C) Ternary complex formed by Cand1-Cul1-Roc1 (Goldenberg et al.; *Cell* **2004**, 119, 517–528).

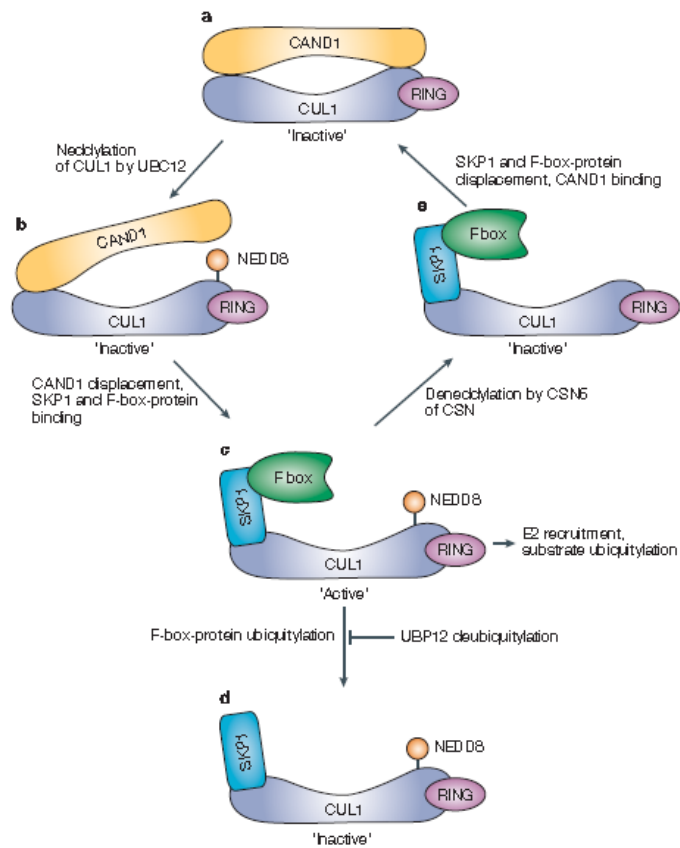


Figure 15. Regulation mechanism of SCF E3 complex activity by the cycle CAND1/Nedd8. (A) SCF complex is inactive as its catalytic core is assembled with CAND1; (B) Neddylated of Cul1 lysine leads to CAND1 dissociation; (C) The catalytic core can assemble with SKP1–F-box substrate-recognition module reconstituting an active complex that is able to ubiquitylate bound substrates; (D) Ubiquitylation and degradation of F-box protein allow association of a new F-box protein with SCF; (E) CSN-mediated deneddylation of SCF might lead to the dissociation of SKP1 and the sequestration of Cul1 by CAND1 (Goldenberg et al.; *Cell* **2004**, 119, 517–528).

2. AIM OF THE PROJECT

As broadly introduced, CA IX is a tumor-associated CA isoform, acting as a negative prognostic factor in many cancer types. Moreover, an increasing number of scientific papers shows an involvement of CA IX in resistance to anticancer drugs. In particular, a recent paper published on the FEBS Journal in 2010 suggests that CA IX may be involved in anticancer drug resistance through its capability to acidify extracellular microenvironment²²⁴.

Because of its selective expression in tumor cells, critical function as pH regulator and cell localization to the membrane, CA IX represents an attractive target for anti-cancer drug design.

At present, two main classes of CA IX inhibitors are under investigations, monoclonal antibodies and small molecule inhibitors. Unfortunately, both classes of inhibitors possess some limitations; monoclonal antibodies reach with difficulty poorly vascularized and hypoxic tumor regions, whereas small molecules are poorly specific because of high degree of homology among the catalytic sites of the various mammalian CAs. So, an important goal would be to design highly selective drugs that inhibit only extracellular CA IX without inhibiting intracellular ones, such as CA II, that is ubiquitous and expressed under physiological conditions.

As the intracellular tail of CA IX was demonstrated to be critical for its membrane localization and ability to acidify the extracellular space, suggesting a possible involvement in protein-protein interactions that drive CA IX towards the plasma membrane and stabilize its correct localization allowing its proper functioning a pH regulator, a winning strategy could be to interfere with such interactions via peptides mimicking CA IX physiological interactors.

So, the aim of this project is to characterize the cellular interactome of this protein, in order to better clarify its biological mechanisms and to identify new molecular targets for design of peptide mimetics.

3. RESULTS

3.1 CA IX expression in normoxic and hypoxic HEK-293 cells

To characterize CA IX interactome I have chosen a biochemical strategy, based on the Strep-Tag System, that allows to purify interactors taking advantages of high affinity binding between Strep-tagged bait protein and Strep-Tactin resin.

A sequence encoding the C-terminal Strep-tag was fused to the full length human CA IX cDNA and the strep-tagged CA IX was overexpressed in the human embryonic kidney cell line HEK-293 under both normoxic and hypoxic conditions.

Correct expression of strep-tagged CA IX was evaluated biochemically, through a western blot analysis on protein lysates from normoxic and hypoxic cells, and by confocal immunofluorescence microscopy on transfected cells grown in both normoxia and hypoxia.

The strep-tagged CA IX produced the typical two bands profile in SDS-PAGE; CA IX bands were clearly up-regulated in hypoxia (**Figure 16A**).

Confocal analysis of CA IX-transfected cells showed that CA IX is present at the plasma membrane and, surprisingly, also in the cytoplasm and in the nucleus, with exclusion of nucleoli. A similar pattern of subcellular distribution was also observed in the hypoxic counterpart, but nuclear and perinuclear staining, accordingly to biochemical up-regulation, was more pronounced and exclusion of nucleoli was decreased (**Figure 16B**).

Strep-tagged protein was also characterized by MALDI-TOF-MS analysis. More specifically, CA IX glycopeptides were analysed, proving the expected occurrence of N- and O- glycosylation at Asn 309 and T78 respectively and consequently correct post-translational modification of CA IX (**Figure 16C**).

3.2 CA IX interactome in normoxic and hypoxic HEK-293 cells

Once verified the correct synthesis, post-translational modification and expression of strep-tagged CA IX, an affinity purification experiment was performed, taking advantage of the Strep-Tag System, on protein extracts from HEK-293 cells transfected with the recombinant protein and grown under both normoxic and hypoxic

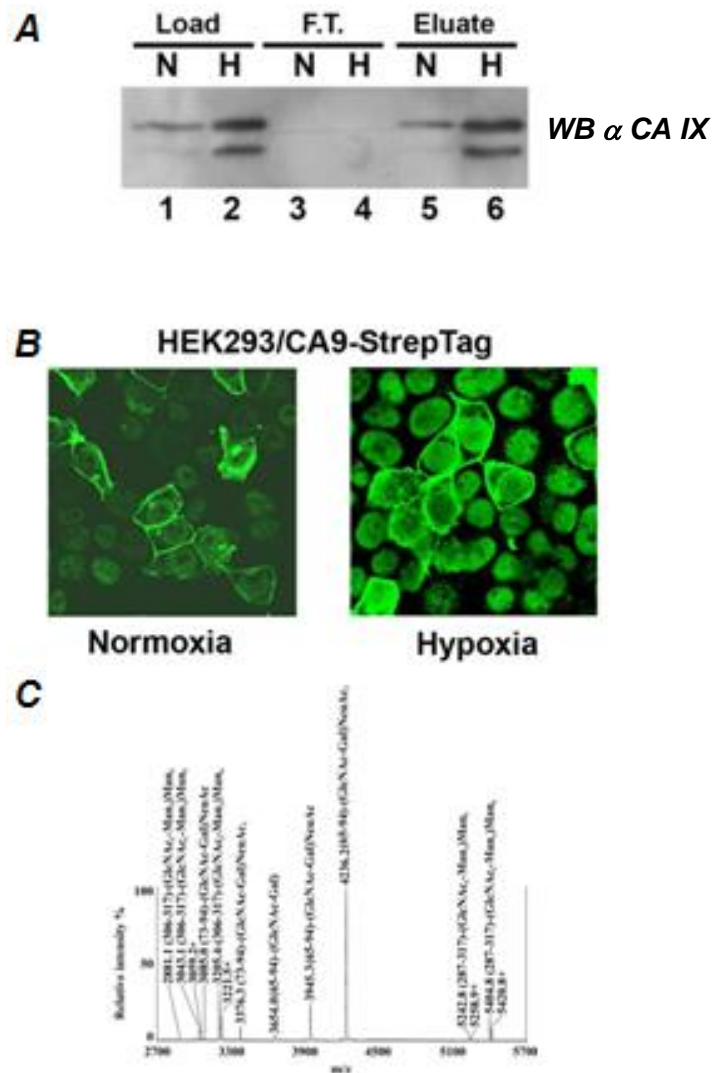


Figure 16. Strep-tagged CA IX expression in HEK-293 cells (A) Western blot analysis of lysates from normoxic (N) and hypoxic (H) HEK-293 cells transfected with the strep-tagged CA IX vector. Protein extracts of lanes 1 and 2 were loaded on Strep-Tactin columns for co-purification of CA IX and its interactors in both normoxic and hypoxic conditions. Flow-through (lanes 3–4) and eluate (lanes 5–6) fractions were probed with a CA IX antibody; (B) Immunofluorescence analysis of recombinant CA IX in normoxic (left) and hypoxic (right) HEK-293 cells; (C) MALDI-TOF analysis on glycopeptides from tagged-CA IX.

conditions. As control sample, to identify non-specifically bound interactors, a protein extract from mock-transfected HEK-293 cells was used. So, tagged CA IX was co-purified with bound interactors. Eluates from mock, normoxic and hypoxic lysates were loaded on a SDS-PAGE gel. After silver staining, each gel lane was cut into 21 similar slices and subjected to nLC-ESI-LIT-MS/MS for protein identifications (Dr. G. Renzone and A. Scaloni, ISPAAM, CNR, Naples) (**Figure 17**).

29, 45 and 72 proteins were identified in the normoxic, hypoxic and mock samples, respectively. A list of potential CA IX interactors was obtained subtracting from normoxic and hypoxic identifications those from mock sample. CA IX putative interactors were 6 for normoxic condition and 25 for hypoxic condition; 3 of them, namely CAND1, CV028 and RS5, were found in both experimental conditions. Electrophoretic analysis of co-purified interactors had already highlighted that a higher number of interactions occurred under hypoxic conditions (**Table 1**).

To better understand physical and structural interactions among the 25 potential interactors of CA IX, I performed a bioinformatic analysis through the tool String 9.0 that is a database for annotation of physical and functional interactions.

CA IX interactors identified from normoxic cells comprise the mitochondrial ATP synthase α/β subunits (ATP5A1 and ATP5B), and Ras GTPase activating protein-binding protein 2 (G3BP2), a scaffold component for mRNA transport. This protein is linked via exportin XPO1 to the main network of CA IX-interacting proteins identified under hypoxia. Interestingly, most of the proteins of this network belong to the nucleocytoplasmic transport machinery, including several members of the importin α (KPNA2), $-\beta$ (IPO4, IPO5, IPO7, IPO9, TNPO1, TNPO3), and exportin (XPO1, XPO2/CSE1L, XPO5, XPOT) families. STRING also highlighted connection of the signal recognition particle receptor subunit β (SRPRB) with the ribosomal protein RPS5 and the catalytic subunit of the tRNA-splicing ligase complex (C22orf28). The latter two CA IX interactors were also found under normoxia. Proteins not connected in the network included the acetyl-CoA carboxylase 1 enzyme (ACACA), the HEAT repeat-containing protein 3 (HEATR3), the mitochondrial trifunctional enzyme subunit alpha (HADHA), the protein SAAL1, and the cullin-associated NEDD8-dissociated proteins 2 and 1 (CAND2 and CAND1), the latter being also found under normoxic conditions (**Figure 18A**).

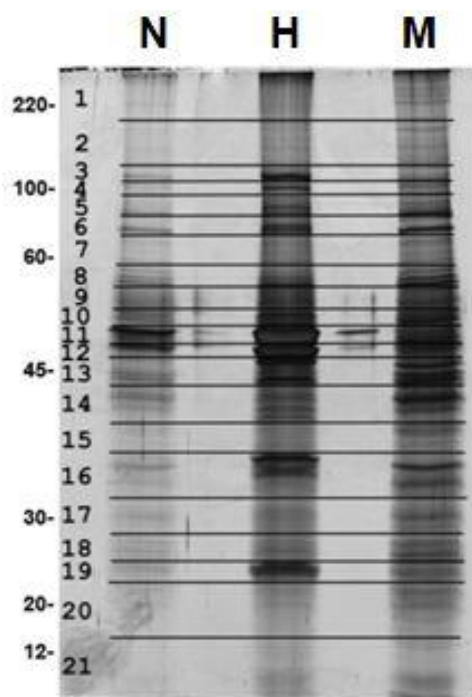


Figure 17. SDS-PAGE analysis of the CA IX interacting proteins in HEK-293 cells. Lysates from normoxic (N) and hypoxic (H) cells transfected with the Strep-tag CA IX vector and from cells transfected with an empty vector were loaded on Strep-Tactin columns for co-purification of CA IX and its binding partners. Eluates were separated on a 10% SDS-PAGE gel and detected by silver nitrate staining: gel bands corresponding to the interactors are those absent in the mock eluate. After staining, each lane was cut into 21 slices to identify interactors by nLC-ESI-LIT-MS/MS analysis.

Accession	Description	Normoxic	Hypoxic
Q16790	Carbonic anhydrase 9, CA9 [CAH9_HUMAN]	X (bait)	X (bait)
Q86VP6	Cullin-associated NEDD8-dissociated protein 1, CAND1 [CAND1_HUMAN]	X	X
Q9UN86	Ras GTPase-activating protein-binding protein 2, G3BP2 [G3BP2_HUMAN]	X	
P25705	ATP synthase subunit alpha, mitochondrial, ATP5A1 [ATPA_HUMAN]	X	
P06576	ATP synthase subunit beta, mitochondrial, ATP5B [ATPB_HUMAN]	X	
Q9Y3I0	UPF0027 protein C22orf28, C22orf28 [CV028_HUMAN]	X	X
P46782	40S ribosomal protein S5, RPS5 [RS5_HUMAN]	X	X
O75155	Cullin-associated NEDD8-dissociated protein 2, CAND2 [CAND2_HUMAN]		X
Q13085	Acetyl-CoA carboxylase 1, ACACA [ACACA_HUMAN]		X
Q96P70	Importin-9, IPO9 [IPO9_HUMAN]		X

Q8TEX9	Importin-4, IPO4 [IPO4_HUMAN]		X
O00410	Importin-5, IPO5 [IPO5_HUMAN]		X
O95373	Importin-7, IPO7 [IPO7_HUMAN]		X
P52292	Importin subunit alpha-2, KPNA2 [IMA2_HUMAN]		X
Q9HAV4	Exportin-5, XPO5 [XPO5_HUMAN]		X
O43592	Exportin-T, XPOT [XPOT_HUMAN]		X
P55060	Exportin-2, CSE1L [XPO2_HUMAN]		X
O14980	Exportin-1, XPO1 [XPO1_HUMAN]		X
Q9Y5L0	Transportin-3, TNPO3 [TNPO3_HUMAN]		X
Q92973	Transportin-1, TNPO1 [TNPO1_HUMAN]		X
Q9UBB4	Ataxin-10, ATXN10 [ATXN10_HUMAN]		X
P00918	Carbonic anhydrase 2, CA2 [CAH2_HUMAN]		X
Q7Z492	HEAT repeat-containing protein 3, HEATR3 [HEATR3_HUMAN]		X
Q96ER3	Protein SAAL1, SAAL1 [SAAL1_HUMAN]		X
Q9Y5M8	Signal recognition particle receptor subunit beta, SRPRB [SRPRB_HUMAN]		X
P40939	Trifunctional enzyme subunit alpha, HADHA [ECHA_HUMAN]		X

Table 1. List of potential binding partners of CA IX in HEK-293 cells. Strep-tagged CA IX from transfected cells grown under both normoxic and hypoxic conditions was used as bait to dock its interactors. Such complexes were bound by Strep-Tactin and, once purified, resolved by SDS-PAGE. Each gel lane was cut into 21 similar slices, which were then treated with trypsin and subjected to nLC-ESI-LIT-MS/MS analysis for protein identification. Aspecifically-bound interactors were excluded subtracting from total protein identifications identifications relative to mock sample.

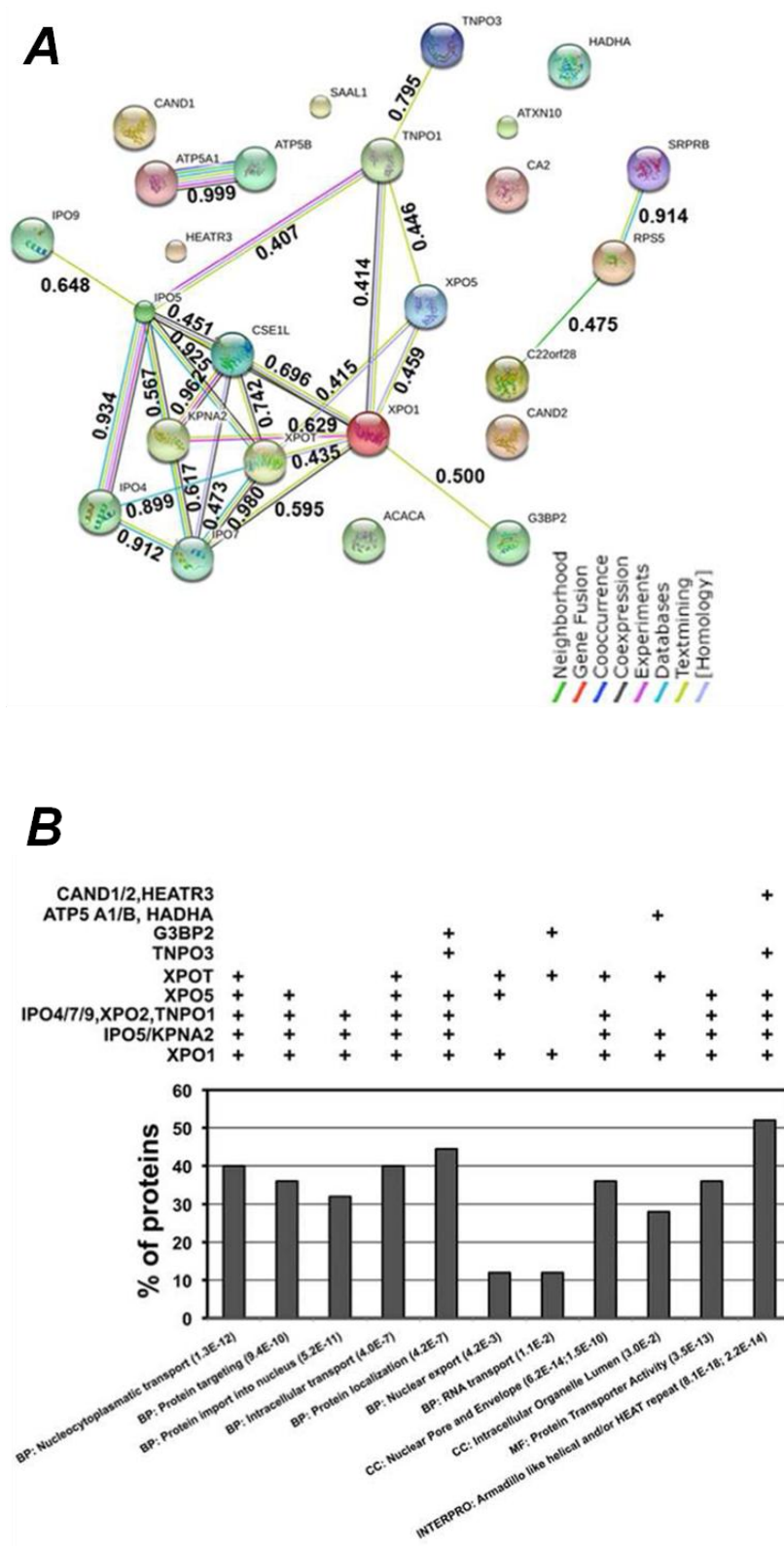


Figure 18. Bioinformatic characterization of CA IX interactors. (A) Identified proteins were subjected to String analysis to highlight possible physical and functional interactions among the 25 interactors of CA IX. Proteins are connected by lines of different colors, according to the color code shown at the bottom. Values close to the lines report the confidence scores, as revealed by functional interaction analysis; (B) Clustering of interactors on the basis of descriptors for biological process (BP), cell compartment (CC), molecular function (MF), or protein family (INTERPRO) suggested by DAVID database.

After String analysis, the potential CA IX interactors were further classified under gene ontology parameters (namely, biological process and INTERPRO) in the DAVID bioinformatic database. This new analysis, besides highlighting that most proteins were obviously involved in nucleocytoplasmic transport of proteins and RNA and located at the NPC/ nuclear envelope, showed that around 50% of potential interactors belonged to the family of the ARM and HEAT repeat containing proteins. The latter include those involved in nucleocytoplasmic transport, as well as CAND1, CAND2 and HEATR3 (**Figure 18B**). As already introduced, members of this family feature the presence of α -helical domains that are usually involved in protein interactions.

3.3 Validation of XPO1, TNPO1 and CAND1 as CA IX interactors

To confirm data emerged from affinity purification experiments and identifications obtained by mass spectrometry analysis, co-precipitation experiments were performed.

XPO1, TNPO1 and CAND1 were selected as representative members of the CA IX interactome. The first two interactions were chosen as representative of the main network of CA IX-interacting proteins, the last, that seems to occur also in normoxia, for the involvement of CAND1 in important biological processes such as regulation of transcription and proteasome-mediated protein degradation.

Results validated all three interactions.

In fact even if all three proteins were equally expressed in total lysates from normoxic and hypoxic transfected cells, they co-precipitated and were only represented under hypoxic conditions in the case of XPO1 and TNPO1, under both normoxic and hypoxic conditions in the case of CAND1.

Since western blotting of the input samples clearly shows that endogenous XPO1, TNPO1, and CAND1 levels do not vary in hypoxia, it can be postulated that increased levels of the endogenous proteins interacting with strep-tagged CA IX may depend on the known overexpression of CA IX in hypoxic cells (**Figure 19**).

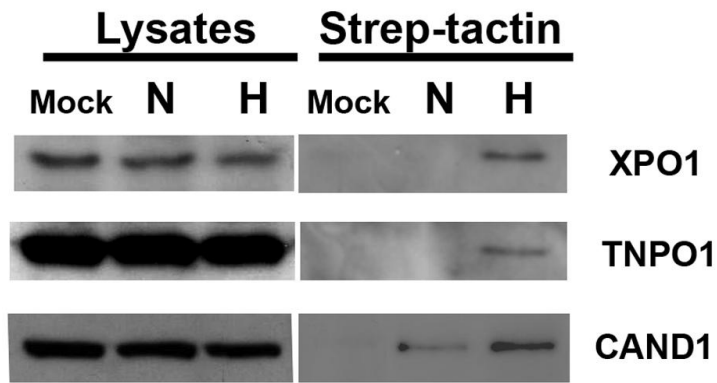


Figure 19. Co-precipitation of CA IX with XPO1, TNPO1 and CAND1. Interactors chosen for validation were affinity precipitated through recombinant CA IX in lysates from normoxic (N) and hypoxic (H) cells transfected with the Strep-tag CA IX vector. As negative control, co-precipitation was also performed on lysates from cells transfected with an empty vector (Mock). Eluates were subjected to western blot analysis and interactors detected by commercial antibodies.

3.4 Identification of the minimal CA IX sequence required for the interaction with XPO1, TNPO1 and CAND1

As most CA IX interactors, identified by interactome analysis, were intracellular proteins, the next step was to investigate the region of the C-terminal intracellular portion of CA IX involved in the binding to XPO1, TNPO1 and CAND1.

So pull-down experiments were performed, using synthetic peptides, reproducing the cytosolic portion of CA IX (434-459), on cellular lysates from HEK-293 cells transfected with strep-tagged CA IX and grown in both normoxia and hypoxia.

Results show that the entire intracellular tail alone is not sufficient to interact with validated interactors XPO1, TNPO1 and CAND1, irrespective of its phosphorylation status (lanes 3 and 4). This prompted us to design longer peptides and allowed us to verify that the minimal region required for interactions with these proteins also requires 16 amino acids of the TM region (418-459). Moreover, phosphorylation of this region at T443 (lane 5) and Y449 (lane 6) leads to a more efficient binding than the non-phosphorylated counterpart (lane 7), even if phosphorylation is important but non crucial for occurrence of interactions. The specificity of the binding was verified by a scrambled C-terminal sequence peptide (lane 2) (**Figure 20**).

3.5 Native complexes of XPO1 and CA IX IN HEK-293 cells

To confirm data emerged from the characterization of CA IX interactome also in cells non transfected with strep-tagged CA IX and so expressing only endogenous protein, I performed an immunoprecipitation experiment to validate the occurrence of XPO1 and CA IX complexes in HEK-293 cells.

Co-IP experiments were performed on cell lysates from HEK-293 cells, grown under both normoxic and hypoxic conditions; XPO1 was co-precipitated through the anti-CA IX monoclonal antibody M75 and revealed in the western blot experiment of **figure 21**, lane 4, only in the hypoxic condition.

This experiment does indeed show the presence of native CA IX complexes in living cells, in which endogenous levels of the two proteins are expressed. Once again, the occurrence of the complexes in the hypoxic condition could be associated to higher expression of CA IX and/or its increased nuclear presence in the hypoxic cells.

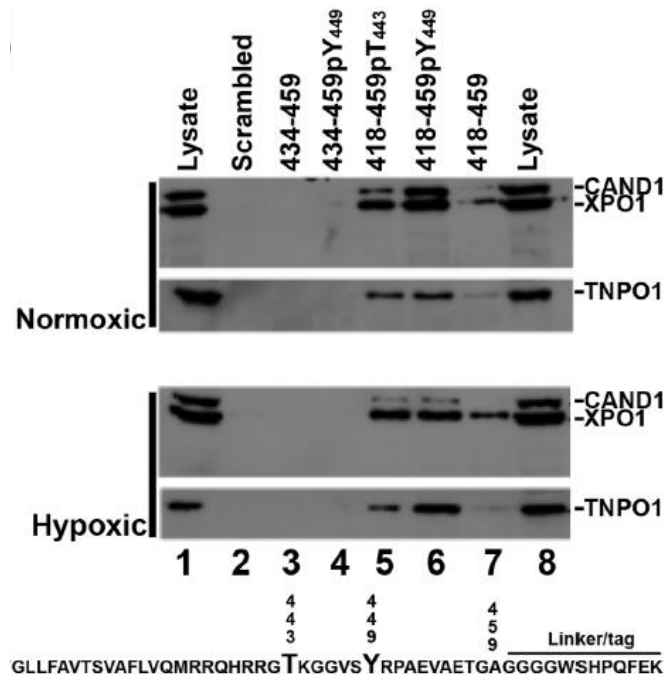


Figure 20. Biochemical characterization of the minimal region required for CA IX interactions. Pull down assays were performed on lysates from normoxic and hypoxic cells transfected with the Strep-tag CA IX vector using synthetic peptides, fused to a C-terminal Strep-tag, reproducing the intracellular tail of CA IX. After a first negative result using the fragment 434-459, both non-modified (lane 3) and phosphorylated (lane 4), the minimal region useful for binding of interactors was recognized in the fragment 418-459 (lanes 5, 6 and 7), encompassing sixteen TM amino acids.

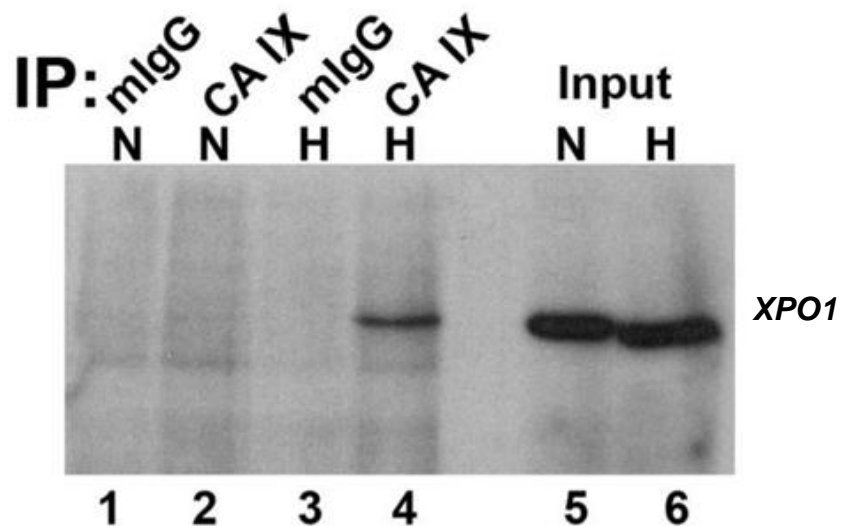


Figure 21. Immunoprecipitation of endogenous CA IX and XPO1 complexes. The CA IX interactors XPO1 was immunoprecipitated together with CA IX through the anti CA IX monoclonal antibody M75 in lysates from normoxic (N, lane 2) and hypoxic (H, lane 4) HEK-293 cells. As negative control, immunoprecipitation was also performed on the same lysates through mouse IgG (lanes 1 and 3). Eluates were subjected to western blot analysis and interactors detected by commercial antibody.

3.6 Analysis of subcellular distribution of CA IX in normoxic and hypoxic HEK-293 cells

CA IX so far has been described mainly as a membrane-bound carbonic anhydrase. However results from characterization of interactome and preliminary data from immunofluorescence analysis of strep-tagged CA IX in HEK-293 cells suggest a more complex localization of this glycoprotein, shown to interact with cytoplasmic and nuclear proteins and to distribute almost uniformly within cells in both normoxia and hypoxia.

Further experiments were then performed in HEK-293 cells to compare distribution of endogenous proteins in normoxia and hypoxia.

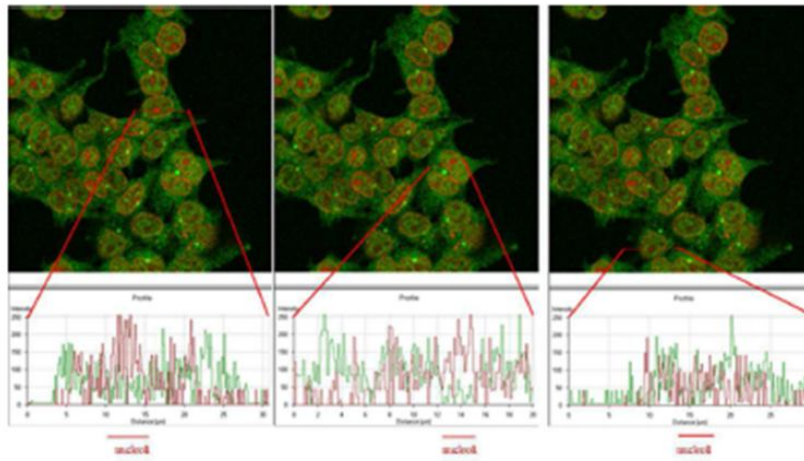
Images corresponding to normoxic cells (upper panel of **figure 22**) show that CA IX (green) gives a diffuse staining and also accumulates in the nucleus, with exclusion of nucleoli; in this condition, membrane staining is also present but membrane CA IX accumulation is limited. The same pattern of distribution was observed in images relative to hypoxic cells (lower panel of **figure 22**), where staining is more pronounced, especially in the nucleus. Moreover, CA IX accumulates in the nucleoli that were excluded in normoxic condition. Interestingly, several cells showed bright fluorescence enrichment in close proximity to the nuclei, compatible with centrosome.

In this experiment possible co-localization of CA IX with XPO1 was also evaluated. Images show that, as expected, XPO1 (red) is located in the nuclear and perinuclear region, with a striking re-distribution to the nuclear envelope and to nucleoli in hypoxic cells. Confirming biochemical data, CA IX and XPO1 co-localize in both nucleoli and perinuclear region under hypoxic conditions, as suggested by the occurrence of yellow signals in the merged images, top and bottom panels on the right.

This distribution is even more evident observing intensity profiles of isolated signals of CA IX and XPO1 in the nucleus and in the nucleoli. In normoxic cells, nuclear CA IX signal is moderate whereas nucleolar one is weak; in these cells, in two out of the three cases, nucleolar XPO1 signal is positive. In hypoxic cells, also nucleolar CA IX signal becomes discrete and that of XPO1 is even stronger.

Nuclear localization of CA IX and its redistribution in nuclear compartments under hypoxia was also confirmed by confocal microscopy experiments on isolated nuclei

Normoxia



Hypoxia

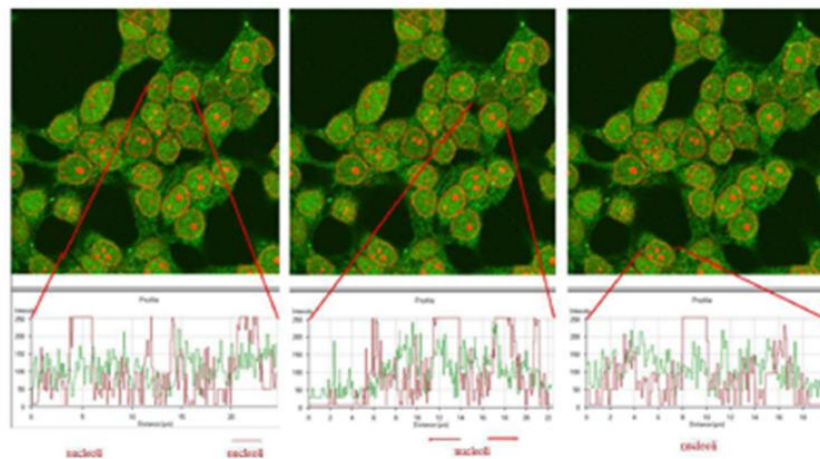


Figure 22. Immunofluorescence analysis of CA IX and XPO1 cell distribution in normoxic and hypoxic HEK-293 cells. Graphics at the bottom show signal intensity of CA IX and XPO1 along red lines that cross nuclei in which nucleoli are more representative.

from normoxic, hypoxic, and DMOG-treated HEK-293-CA9 cells constitutively expressing the full-length CA IX protein. DMOG treatment is an example for a chemically induced hypoxia. Isolated nuclei were highlighted by DAPI. CA IX staining (green) appeared with a punctuate pattern in perinuclear compartments of normoxic cells (upper panel of **Figure 23**); conversely, strong CA IX signals were easily appreciated in hypoxic cells (middle panel of **Figure 23**), both in DAPI-stained nuclear compartments and in DAPI-excluded nucleoli. Under chemical hypoxia (lower panel of **Figure 23**), an evident CA IX staining was also represented in the DAPI-excluded nucleoli. It is worth noting that in all tested conditions, the isolated nuclei showed perinuclear enrichments of CA IX staining compatible with centrosome localization. Altogether, these results support the existence of a hypoxia-driven molecular mechanism regulating the increased expression of CA IX and its enriched presence in nuclear, nucleolar, and perinuclear compartments.

3.7 Identification and analysis of putative NES and NLS in CA IX sequence

To understand how CA IX interacted with XPO1 and TNPO1, a bioinformatic analysis of the minimal region required for these interactions was performed, in order to evaluate the presence of putative NES and NLS sequences in the CA IX C-terminal region.

The putative NES has been found using the software NetNES; it consists in a hydrophobic region, leucine-rich, that may be involved in interactions with exportins, and specifically correspond to the sequence ILALVFGL (415-422) (**Figure 24A**). Instead, a putative NLS was found through the software NLStradamus; it consists in a basic motif corresponding to the sequence RRGHRRGTKGG (436-446) (**Figure 24B**).

To evaluate whether these two putative sequences were functional NES and NLS sequences, their ability to affect the subcellular distribution of a GFP protein reporter was tested. To this purpose, several fusion constructs in which GFP was in-frame fused at the C-terminus with canonical and putative NES/NLS sequence, were generated and transfected in HEK-293 cells, to be analysed by confocal immunofluorescence microscopy (**Figure 25**).

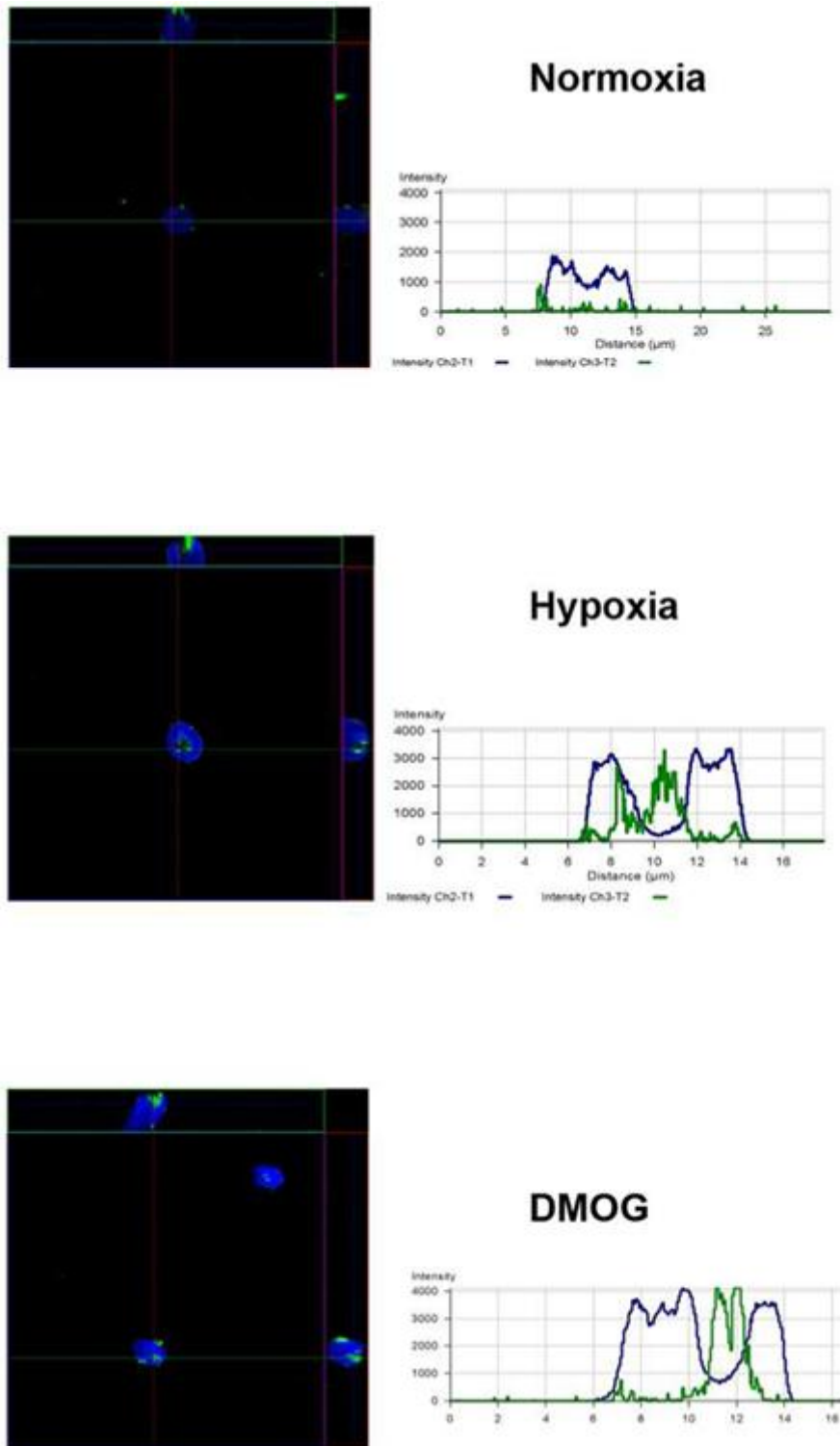
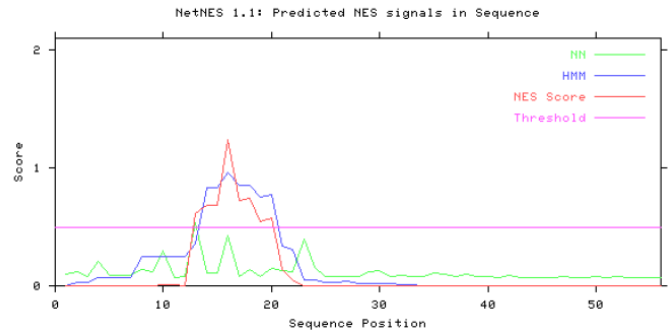


Figure 23. Immunofluorescence analysis of nuclei isolated from HEK-293-CA IX cells. Nuclei isolated from HEK-293-CA IX cells were fixed and stained with DAPI (blue) and with CA IX specific antibody (green). Merged images were converted to graphs representing the intensity profiles of DAPI and CA IX-related signals across the nuclei.

A

CENTER FOR BIOLOGICAL SEQUENCE ANALYSIS CBS	NetNES 1.1 Server - prediction results Technical University of Denmark
---	---

>Sequence - NetNES 1.1 prediction



#Seq-Pos-Residue	ANN	HMM	NES	Predicted
#-----				
Sequence-1-P	0.097	0.000	0.000	-
Sequence-2-V	0.115	0.028	0.000	-
Sequence-3-Q	0.078	0.028	0.000	-
Sequence-4-L	0.208	0.071	0.000	-
Sequence-5-N	0.085	0.071	0.000	-
Sequence-6-S	0.089	0.071	0.000	-
Sequence-7-C	0.090	0.071	0.000	-
Sequence-8-L	0.141	0.244	0.000	-
Sequence-9-A	0.115	0.244	0.000	-
Sequence-10-A	0.301	0.244	0.008	-
Sequence-11-G	0.071	0.244	0.006	-
Sequence-12-D	0.076	0.244	0.003	-
Sequence-13-I	0.535	0.356	0.615	Yes
Sequence-14-L	0.105	0.837	0.688	Yes
Sequence-15-A	0.109	0.837	0.687	Yes
Sequence-16-L	0.426	0.959	1.235	Yes
Sequence-17-V	0.084	0.850	0.728	Yes
Sequence-18-F	0.135	0.851	0.740	Yes
Sequence-19-G	0.084	0.756	0.545	Yes
Sequence-20-L	0.152	0.773	0.570	Yes
Sequence-21-L	0.131	0.336	0.138	-
Sequence-22-F	0.122	0.306	0.048	-
Sequence-23-A	0.399	0.051	0.000	-
Sequence-24-V	0.163	0.053	0.000	-
Sequence-25-T	0.078	0.028	0.000	-
Sequence-26-S	0.082	0.028	0.000	-
Sequence-27-V	0.082	0.036	0.000	-
Sequence-28-A	0.076	0.023	0.000	-
Sequence-29-F	0.116	0.023	0.000	-
Sequence-30-L	0.126	0.020	0.000	-
Sequence-31-V	0.076	0.016	0.000	-
Sequence-32-Q	0.085	0.015	0.000	-
Sequence-33-M	0.084	0.015	0.000	-
Sequence-34-R	0.079	0.000	0.000	-
Sequence-35-R	0.109	0.000	0.000	-
Sequence-36-Q	0.096	0.000	0.000	-
Sequence-37-H	0.084	0.000	0.000	-
Sequence-38-R	0.097	0.000	0.000	-
Sequence-39-R	0.082	0.000	0.000	-
Sequence-40-G	0.080	0.000	0.000	-
Sequence-41-T	0.074	0.000	0.000	-
Sequence-42-K	0.091	0.000	0.000	-
Sequence-43-G	0.073	0.000	0.000	-
Sequence-44-G	0.068	0.000	0.000	-
Sequence-45-V	0.070	0.000	0.000	-
Sequence-46-S	0.065	0.000	0.000	-
Sequence-47-Y	0.077	0.000	0.000	-
Sequence-48-R	0.072	0.000	0.000	-
Sequence-49-F	0.072	0.000	0.000	-
Sequence-50-A	0.075	0.000	0.000	-
Sequence-51-E	0.068	0.000	0.000	-
Sequence-52-V	0.075	0.000	0.000	-
Sequence-53-A	0.071	0.000	0.000	-
Sequence-54-E	0.073	0.000	0.000	-
Sequence-55-T	0.068	0.000	0.000	-
Sequence-56-G	0.073	0.000	0.000	-
Sequence-57-A	0.074	0.000	0.000	-
//				

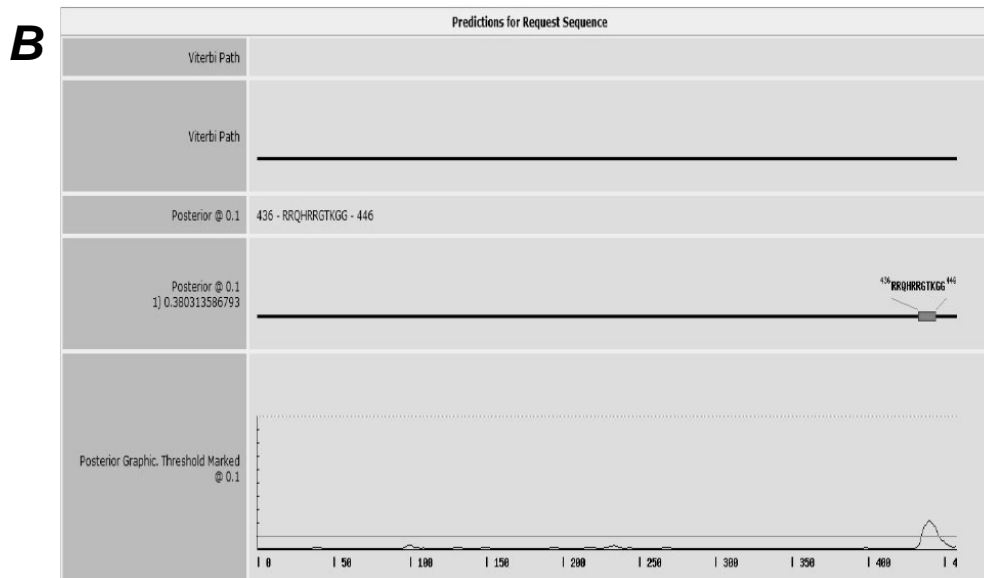


Figure 24. Bioinformatic analysis of CA IX (A) A putative NES sequence has been predicted by NetNES in the transmembrane region (<http://www.cbs.dtu.dk/services/NetNES/>); (B) A putative NLS sequence has been predicted by NLStradamus in the intracellular tail (<http://www.moseslab.csb.utoronto.ca/NLStradamus/>).

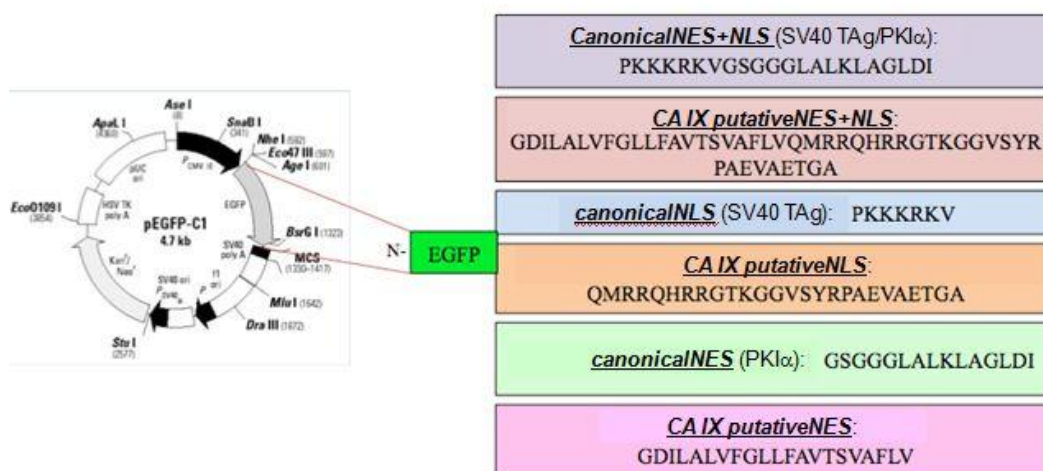


Figure 25. GFP Fusion constructs. GFP was in-frame fused at the C-terminus with the following sequences: canonical NES+NLS, CA IX putative NES+NLS, canonical NLS, CA IX putative NLS, canonical NES, CA IX putative NES.

Pattern of subcellular distribution of GFP obtained from each canonical construct was compared with that obtained from the corresponding putative one and with the normal pattern of subcellular distribution of GFP alone.

Correct expression and expression levels of fusion proteins have been verified through western blot analysis.

Cells were fixed and analyzed by confocal microscopy 24 hours upon transfection.

Images show that in cells transfected with GFP alone there is both a nuclear and a cytosolic staining in the absence of nuclear or cytosolic enrichments. An analogous pattern of expression is shown by cells under both normoxia and hypoxia (**Figure 26A**); cells expressing the fusion protein GFP_NLS, either canonical or CA IX putative, showed a strong nuclear and nucleolar staining, with a weaker cytosolic staining, more evident in normoxic cells transfected with the GFP_CA IX putative NLS construct (**Figures 26 B and C**). Cells transfected with the GFP_canonicalNES+NLS construct showed an impaired nuclear and nucleolar staining and an intense cytosolic staining, that was even more evident in hypoxic cells (**Figure 26 D**). Cells transfected with the CA IX putative NES+NLS construct were characterized by a perinuclear GFP accumulation. In this last case normoxic and hypoxic cells behave in a similar way, but, because of a low efficiency of transfection, images relative to hypoxic condition were not taken (**Figure 26 E**).

Cells transfected with fusion constructs containing the NES sequences were subjected to treatment with Leptomycin B for 4 hours and then fixed and analysed, to the aim of understanding whether this inhibitor of the XPO1-dependent export was actually able to determine GFP accumulation in the nucleus.

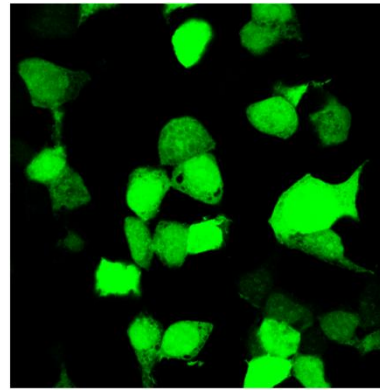
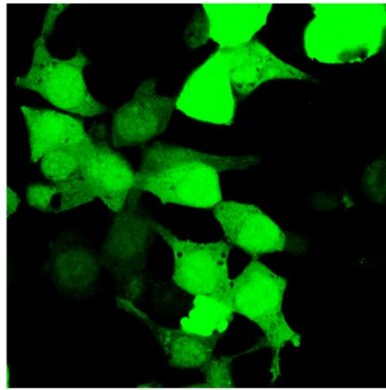
Images show that in cells expressing the fusion protein GFP_NES, regardless of whether sequence was that canonical or putative one, staining was exclusively cytosolic and nuclei seemed to be empty. In both cases treatment with Leptomycin B was able to increase nuclear staining but not nucleolar one (**Figure 27**). Altogether, these results indicate that the putative NES and NLS CA IX sequences are really able to drive a reporter protein, such as GFP, in the nucleus and nucleoli (NLS) or in the cytoplasm (NES). Moreover NES sequence is sensitive to treatment with Leptomycin B. In the presence of both NES and NLS sequences, the nuclear export of the fusion proteins seems to be dominant over the nuclear accumulation.

Normoxia

Hypoxia

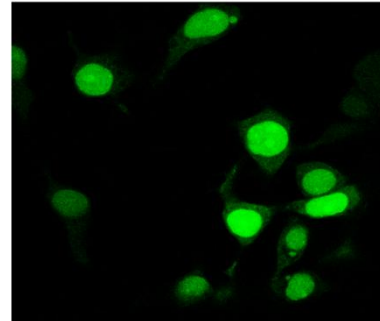
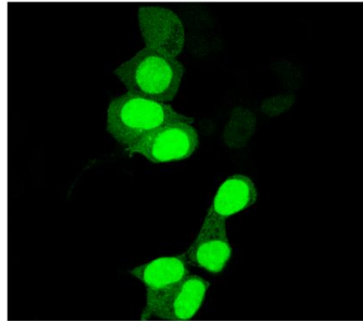
GFP

A



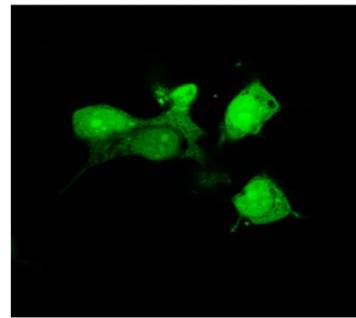
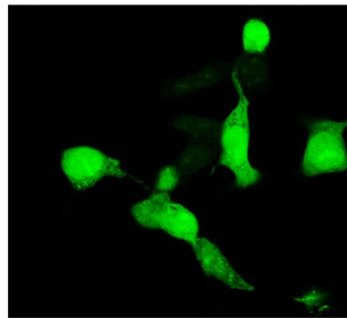
GFP_canonicalNLS

B



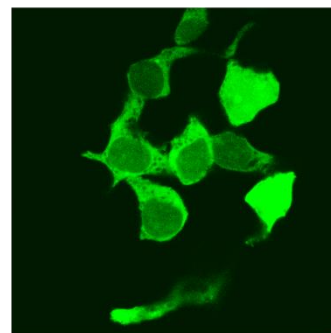
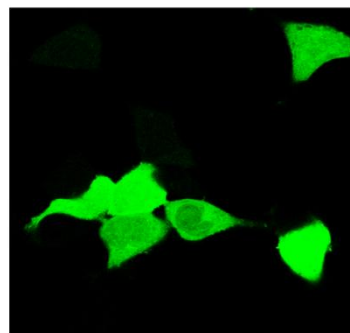
GFP_CA IX putativeNLS

C



GFP_canonicalNES+NLS

D



GFP_CA IX putative NES+NLS

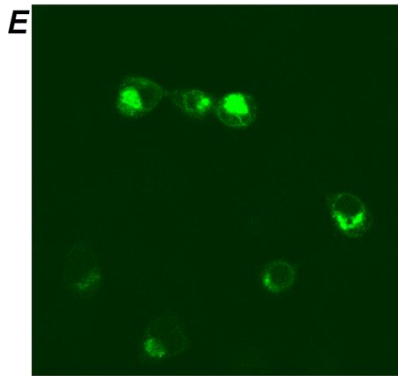


Figure 26. Subcellular localization of NLS and NES+NLS sequences of CA IX in HEK-293 cells. (A) Cells transfected with constructs encoding GFP, (B) GFP_canonicalNLS, (C)GFP_CA IX putative NLS, (D) GFP_canonical NES+NLS, (E) GFP_CA IX putative NES+NLS were grown under normoxia (left panels) or subjected to hypoxic treatment, 24h upon transfection, for 6h (right panels).

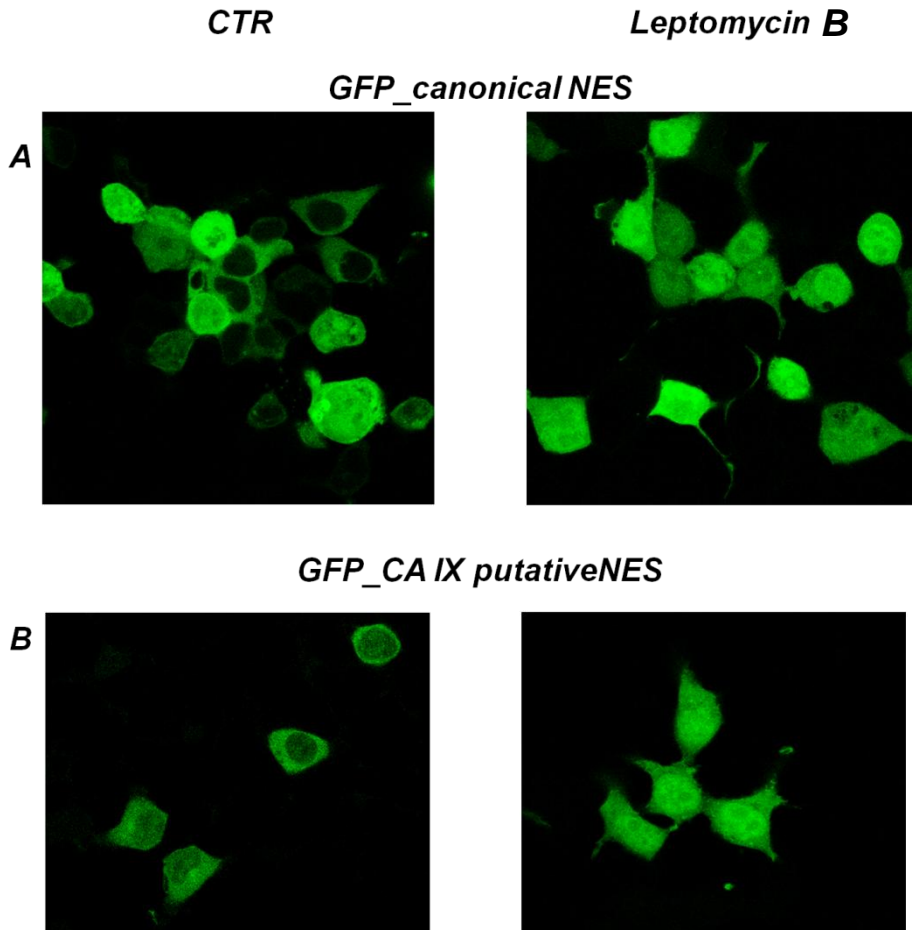


Figure 27. Subcellular localization of NES sequence of CA IX in HEK-293 cells. (A) Cells transfected with constructs encoding GFP_canonicalNES and (B) GFP_CA IX putativeNES were treated with 70% methanol (left panels) or with Leptomycin B, 24h upon transfection, for 4h (right panels).

3.8 Comparison of subcellular distribution of CA IX among different cell lines

To better clarify localization of CA IX in “non-manipulated” and basally CA IX expressing cell models, subcellular distribution of endogenous protein, under normoxic conditions, was evaluated in four cell lines of different tissue origin by confocal immunofluorescence microscopy.

Specifically analysis was carried out in the human colon adenocarcinoma cell line GEO, in the human embryonic kidney cell line HEK-293, in the human neuroblastoma cell line SH-SY5Y and finally in the immortalized human fibroblast cell line BJ5T α .

According with data available in literature about increased expression of CA IX in high density cell cultures⁴⁹, images show that CA IX is expressed almost exclusively at the plasma membrane only in the GEO cells, where a weak perinuclear or nuclear staining is anyhow detectable, whereas, surprisingly, it accumulates in the nucleus and, to a lesser degree, in the cytoplasm and at the plasma membrane in the other cell lines, confirming pattern of cell distribution showed by transfected cells for recombinant protein (**Figure 28**).

3.9 *In vivo* expression and localization of CA IX

Finally, to further deepen pattern of CA IX expression in cancer disease, seven cases of clear cell renal cell carcinomas (ccRCC) were analysed by immunohistochemical analysis.

Here I show four representative samples (**Figure 29**).

In each of them CA IX was mainly detected at the cell membrane and often co-detected in the cytosol. Moreover two out of the seven specimens also showed a nuclear localization for CA IX (lower panels C and D). In these cases, nuclear reactivity for CA IX was associated with cancer tissue districts containing tightly linked neoplastic cells and a limited fibrovascular network, suggesting its possible relationship to physiological hypoxia.

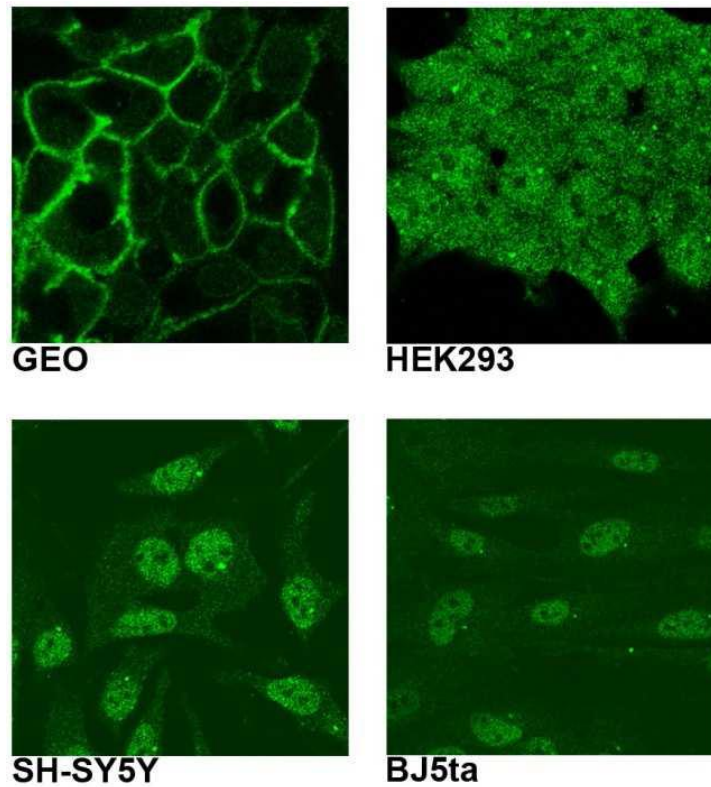


Figure 28. Subcellular distribution of CA IX in some human cancer cell lines. GEO (colon adenocarcinoma), HEK-293 (embryonic kidney carcinoma), SH-SY5Y (neuroblastoma) and BJ5T α (telomerase immortalized fibroblasts) cells were fixed and permeabilized to detect CA IX (green). In GEO cells is shown the best known membrane localization of CA IX, whereas in the other cell lines CA IX is broadly distributed, with a positive staining of nuclei.

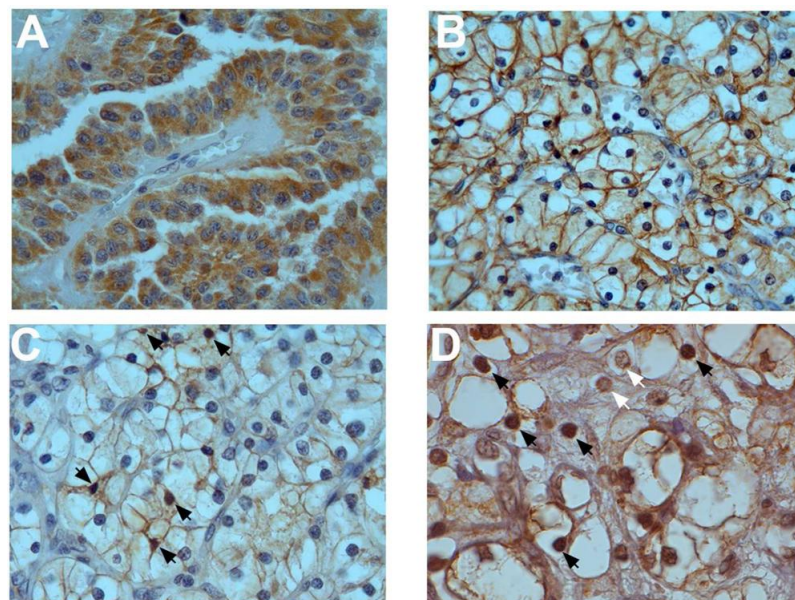


Figure 29. Immunohistochemical analysis of CA IX expression in clear cell renal cell carcinoma (ccRCC). In all four ccRCC cases, CA IX is mainly detected at the cell membrane and often co-detected in the cytosol. In two (lower panels C and D) out of the seven specimens, CA IX also showed a nuclear localization.

3.10 Functional validation of CA IX-CAND1 interaction

To investigate a possible functional significance of interaction between CA IX and CAND1 I attempted to generate cell clones stably expressing low levels of CAND1 protein through RNA interference technology.

Three different shRNA constructs, potentially able to interfere with CAND1 mRNA expression, namely sh2454, sh2555 and sh2562, were transfected in HEK-293 cells; a pool of clones interfered with CAND1 was obtained from each construct.

Interference efficiency was evaluated through western blot analysis on cell lysates from the different pools. Results showed that the sh2555 and sh2562 constructs (lane 3 and 4, respectively) were more efficient in interfering with CAND1 mRNA expression than sh2454 construct (lane 2) (**Figure 30**).

As already introduced, CAND1 is involved in regulation of protein stability through inhibition of assembly of SCF E3 ubiquitin ligase complex, that targets protein for degradation by 26S proteasome. To investigate if CAND1 was involved in CA IX stabilization, I evaluated by western blotting CA IX protein levels in cell lysates from HEK-293 clones stably interfered with CAND1.

Results of analysis show that there is a parallel decrease in CA IX protein level in clones interfered with CAND1 (lane 2 and 3) in comparison to clones interfered with a non silencing construct (shNS) (lane 1). This datum strongly supports initial hypothesis that CA IX is a target of the Ubiquitin-Proteasome Pathway (UPP) and is positively regulated by CAND1, so suggesting that a functional interaction between CA IX and CAND1 occur and may responsible of high stability of CA IX protein (**Figure 31**).

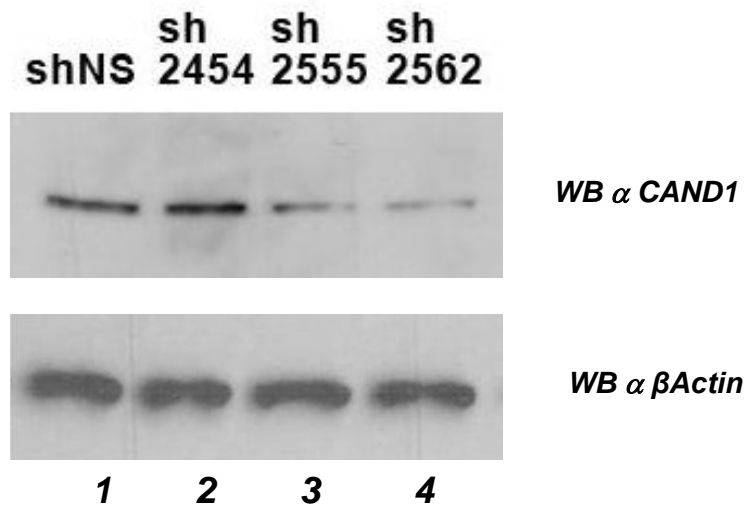


Figure 30. Western blot analysis on lysates from stable HEK-293 pools of clones expressing shRNAs targeting CAND1 mRNAs. shRNAs 2555 and 2562 are able to stably interfere with CAND1 expression in the generated pool of clones.

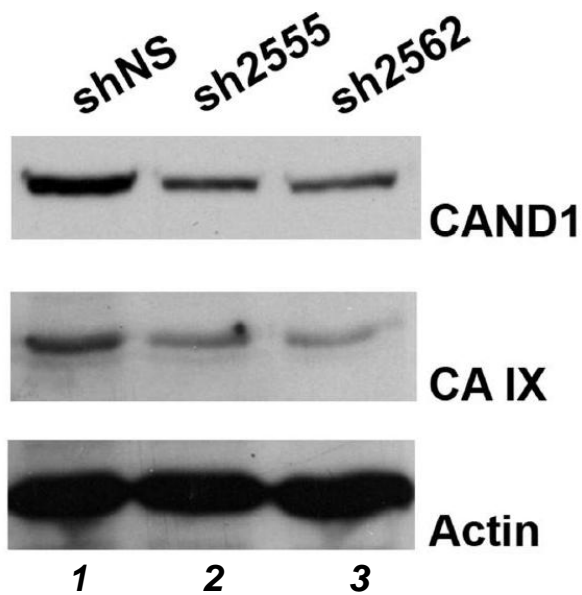


Figure 31. Western blot analysis on lysates from HEK-293 cells stably expressing the shRNAs 2555 and 2565. In HEK-293 clones interfered with CAND1 expression through the shRNAs 2555 and 2562 a parallel decrease in CA IX expression is associated to down-regulation of CAND1.

4. MATERIALS AND METHODS

4.1 Cell lines and experimental treatments

The HEK-293, SH-SY5Y, BJ5T α and GEO cell lines were purchased from ATCC. Cells were cultured in DMEM containing 10% fetal bovine serum (Euroclone) and penicillin/streptomycin, at 37°C, in 5% CO₂ humidified atmosphere.

Transient transfection of HEK-293 cells with the empty vector, pRcCMV, or the strep-tagged CA IX vector have been performed at a confluence of 70% using the calcium phosphate method. At 24 hours after transfection some cells were maintained under normoxic conditions while other were subjected to hypoxic treatment, for sixteen hours, in an incubator with N₂ atmosphere containing 2% O₂ and 5% CO₂.

HEK-293 cells for analysis of putative NES and NLS CA IX sequences were transfected with the same method. 24 hours upon transfection cells transfected with the constructs containing the NLS or NES+NLS sequences were grown in hypoxia for six hours or maintained under normoxic conditions, while cells transfected with the constructs containing the NES sequences were treated for 4 hours with 20ng/mL of Leptomycin B (Sigma Aldrich) or, as control, with 70% methanol, that is the solvent in which is solved Leptomycin B.

Analogously HEK-293 cells were transfected with pSM2 vectors containing shRNAs targeting CAND1 mRNAs to interfere their expression. Stable clones were established by treating cells for two weeks with 2 μ g/ml of puromycin and amplified using 0, 25 μ g/ml of puromycin to maintain stable expression of constructs.

4.2 DNA constructs

The expression construct encoding the full-length CA IX protein was obtained by RT-PCR amplification of mRNA isolated from non small cell lung cancer explanted tumors with ImProm-II Reverse transcriptase (Promega) and Pfu DNA polymerase. The primers for cDNA amplification were synthesized at CEINGE oligonucleotide facility and were the following: ca9for, 5'-cacaagcttagccgcatggctcccctgtgccccagc-3'; ca9rev, 5'-cactctagattatcctcctccttttgaactgcgggtggctccaggctccatctcggctacctc-3'. This last oligonucleotide contained additional bases encoding for the Strep-tag II

sequence WSH PQFEK, through which recombinant protein was tagged. The PCR product was cloned in the pRcCMV vector (Invitrogen). cDNA was fully sequenced for verification.

Constructs containing NLS, NES+NLS and NES sequences, canonical and CA IX putative, were generated in frame-fusing them at the C-terminus of EGFP in the vector of expression pEGFP_C1.

The construct pEGFP_NLS-SV40 (TAg) was generated through annealing of the following synthetic oligonucleotides: NLS_SV40 (TAg) _US: 5'-GATCTCCAAAAAAGAAGAGAAAGGTAG-3'; NLS_SV40 (TAg) _LS: 5'-TCGACTACCTTTCTCTTCTTTTTTGGGA-3';

The construct pEGFP_canonicalNES+NLS was produced using a synthetic forward oligonucleotide as template and a reverse oligonucleotide as primer to copy the template: NES_NLS_can_US: 5'-ATAAGATCTCCAAAAAAGAAGAGAAAGGTAGGATCCGGCGGCGGCTTAGCCTTGAAATTAGCAGGTCTTGATATC-3'; NES_NLS_can_Rev: 5'-ACTGTAGTCGACGATATCAAGACCTGCTAATTTTC-3'.

The construct pEGFP_NES-PKIA was generated as described above for NLS, using the following oligonucleotides: NES_PKIA_US: 5'-GATCTTTAGCCTTGAAATTAGCAGGTCTTGATATCG-3'; NES_PKIA_LS: 5'-TCGACGATATCAAGACCTGCTAATTTCAAGGCTAAA -3';

Finally the constructs pEGFP_CA IX putativeNLS and pEGFP_CA IX putativeNES+NLS, encompassing sequence from 434 to 459 and from 412 to 459 of the full length protein, respectively, were generated by PCR from cDNA of full length CA IX using the following oligonucleotides: CA9_Cterm_For: 5'-ATAAGATCTGGTGACATCCTAGCCCTGGT-3'; CA9_Cterm_Rev: 5'-ACTGTAGTCGACGGCTCCAGTCTCGGCTACCT-3'; CA9_IC_For: 5'-ATAAGATCTCAGATGAGAAGGCAGCACAGA-3'; CA9_Cterm_Rev: 5'-ACTGTAGTCGACGGCTCCAGTCTCGGCTACCT-3'.

Differently the construct pEGFP_CA IX putativeNES, including CA IX sequence from 410 to 435, was produced by annealing of the following synthetic oligonucleotides: CA9_NES_FWD: 5'-GATCTGCTGGTGACATCCTAGCCCTGGTTTTTGGCCTCCTTTTTGCTGTCACCA

GCG-3'; CA9_NES_RV: 5'-
TCGACGCTGGTGACAGCAAAAAGGAGGCCAAAAACCAGGGCTAGGATGTCACC
AGCA -3'

Forward oligonucleotides contained the restriction site for BglII, whereas reverse oligonucleotides possessed the restriction site for Sall. They have been synthesized at CEINGE oligonucleotide facility and fully sequenced for verification.

The pSM2 vectors containing the shRNAs 2454 (5'-TGCTGTTGACAGTGAGCGACCGTTTGTCTGCAAGAAATATAGTGAAGCCACAGATGTATATTTCTTGCAGGACAAACGGCTGCCTACTGCCTCGGA-3'), 2555 (5'-TGCTGTTGACAGTGAGCGCGCAATGTAGATGATGATGAATTAGTGAAGCCACAGATGTAATTCATCATCATCTACATTGCATGCCTACTGCCTCGGA-3') and 2562 (5'-TGCTGTTGACAGTGAGCGCCCTCATGTTTCTACCATTATATAGTGAAGCCACAGATGTATATAATGGTAGAAACATGAGGATGCCTACTGCCTCGGA-3'), targeting CAND1 mRNAs, together with the non silencing shNS construct, were selected from a library of shRNAs generated by Dr. Greg Hannon at Cold Spring Harbor Laboratory (CSHL) and provided us by the Open Biosystems. These shRNAs were designed to be expressed as human microRNA-30 (miR30) primary transcripts to increase Drosha and Dicer processing of the expressed hairpins and consequently knockdown efficiency. Briefly the hairpin stem consists of 22-nt of dsRNA, complementary to mRNA target, the loop is formed by 19-nt from human miR30; the 125-nt of flanking sequence on either side of the hairpin are also from miR30.

The 22-nt dsRNA portion of all three shRNAs targeting CAND1 mRNAs is complementary to sequences present in the coding region.

4.3 Cell lysates preparation, interactome characterization and mass spectrometry protein identification

Cell lysates were generated by lysis in a buffer containing 50 mM Tris-HCl, 150 mM NaCl, 0,5% Triton X-100, 10% glycerol, pH 7.5, 50 mM NaF, 1 mM Na₃VO₄, 1 mM DTT, 0,4 mM EDTA, pH 8.0, and a mixture of protease inhibitors (Sigma Aldrich)²²⁵. Lysates were clarified by centrifugation at 12,000 g for 20 min at 4 °C and quantified

using BioRad Protein Assay, based on the Bradford method, following the manufacturer's instructions.

Each lysate (2 mg) was challenged with 250 μ L of Strep-Tactin resin (IBA), and incubated for 12 h, at 4 °C. After washing, proteins were eluted with 100 mM Tris-HCl, 150 mM NaCl, 1 mM EDTA, 0.1% Triton X-100, 2 mM D-biotin, pH 8.

Interactors eluted with CA IX were analyzed by 12% SDS-PAGE (14 cm \times 16 cm \times 0.75 mm) in an SE600 vertical electrophoresis system (Hoefer), at 18 °C, using a constant current setting of 25 mA and a maximum of 150 V.

Detection of proteins was performed by silver nitrate staining. Gel images were scanned by the Image Scanner III (GE Healthcare) apparatus and analyzed by the Image Master 2D Platinum 6.0 software (GE Healthcare), according to the manufacturer's instructions.

Each of the three gel lanes from SDS-PAGE was cut and subdivided into 21 similar slices, which were then processed for downstream protein identification by mass spectrometry. Peptide digests of interactors as well as CA IX glycopeptides and phosphopeptides were analyzed by nLC-ESI-LIT-MS/MS. The latter were also analyzed by MALDI-TOF-MS. MS analysis was performed by Dr. G. Renzone and A. Scaloni, ISPAAM, CNR, Naples, as described in detail⁶⁶.

4.4 Bioinformatic analysis

Proteins identified by nLC-ESI-LIT-MS/MS were analyzed using the String v. 9.0 database (<http://string-db.org/>) to discover functional interaction between them²²⁶.

A classification of the identified proteins under parameters of gene ontology was performed through the web-accessible DAVID (v 6.7) annotation system (<http://david.abcc.ncifcrf.gov/home.jsp>)^{227, 228}.

A bioinformatic analysis of CA IX C-terminal region to find putative NES and NLS sequences was performed using the predictive software NetNES 1.1 Server (<http://www.cbs.dtu.dk/services/NetNES/>) and NLStradamus (<http://www.moseslab.csb.utoronto.ca/NLStradamus/>²²⁹), respectively.

4.5 Antibodies, interaction assays and western blot analysis

Antibodies used in experiments described in this thesis were the following: CA IX VII/20 and M75, mouse monoclonals²³⁰; CA IX, rabbit polyclonal (H-120, Santa Cruz Biotechnology); XPO1 (CRM1 C-20, Santa Cruz Biotechnology), goat polyclonal; TNPO1 (karyopherin β 2 F-6, Santa Cruz Biotechnology), mouse monoclonal; CAND1 (TIP120A 48, Santa Cruz Biotechnology), mouse monoclonal.

Affinity purification experiments were performed on 1mg of protein extracts on Strep-Tactin resin for 2 hours, at 4°C. Elution was preceded by 5 washes with lysis buffer. Eluates were analyzed by 10% SDS-PAGE.

Pull down experiments were carried out using synthetic peptides²³¹. Protocol provides for two sequential incubations at 4°C: the first occurs between peptides (0, 5nmol each) and strep-Tactin resin (10 μ l); the second between peptides bound to resin and protein extracts (500 μ g). Proteins specifically bound to resin through peptides and eluted from the resin were determined by western blot analysis. Filters were probed with the XPO1, TNPO1 and CAND1 antibodies.

Co-immunoprecipitation experiments for analysis of CA IX-XPO1 native complexes were performed using an anti- CA IX antibody; immunocomplexes were captured by protein A/G plus agarose (Santa Cruz Biotechnology) and, once eluted, subjected to western blot analysis.

4.6 Fluorescence and immunofluorescence analyses

Immunofluorescence experiments were performed on HEK-293, SH-SY5Y, GEO and BJ5T α cells.

Cells used for analysis were plated on glass slides and, after being subjected to various treatments described in previous sections, fixed with 3% (w/v) paraformaldehyde, 1% (w/v) sucrose in PBS for 15 min and permeabilized with 0.3% (w/v) Triton X-100 in PBS for 3 min, at 4 °C. Cells were then incubated with appropriate dilutions of primary antibodies: CA IX VII /20, mouse monoclonal; XPO1, goat polyclonal. To visualize by fluorescence target protein, cells were incubated for 1h at 25°C with the following secondary antibodies: Texas Red-conjugated donkey anti-goat; Alexa-488-conjugated rabbit antimouse (Jackson Laboratories).

An immunofluorescence analysis was also performed on the isolated nuclei from HEK-293-CA9 cells. Cells were resuspended in 0.1% Tween-20 in PBS and spun at 13 000 × g for 15 min, at 4 °C. After two washes in PBS, the isolated nuclei in the pellet were fixed on polylysine slides (Thermo Scientific) with ice-cold methanol and analyzed using anti-CA IX antibody VII/20, followed by Alexa Fluor 488 donkey antimouse IgG (Invitrogen). The nuclei were stained with DAPI.

For fluorescence analysis on HEK-293 cells transfected with the constructs containing GFP fused at the C-terminus with CA IX NES and NLS sequences under investigation, a transient transfection has been performed. After treatment with Leptomycin B, cells were fixed with 3% (w/v) paraformaldehyde, 1% (w/v) sucrose in PBS for 20 minutes at room temperature (RT).

4.7 Immunohistochemical analysis

Immunohistochemical analysis was performed on seven archived formalin-fixed tissue blocks from ccRCC patients. From each block, 5 µm-thick sections were obtained. They were dewaxed and rehydrated with graded ethanol concentrations. Before staining, sections first were incubated in citrate buffer pH 6, for 45 min, at 97°C, and then in 3% H₂O₂/methanol for 10 min to block endogenous peroxidase activity. Non-specific sites were blocked by background reducing components (DAKO), for 30 min, at room temperature. Tissue sections were incubated at room temperature with primary antibody (CA IX H-120) at 1:50 dilution, for 1 h. Staining was performed with LSAB+System-HRP (DAKO) and diaminobenzidine chromogen (DAKO). Tissue sections were counterstained with Mayer's hematoxylin and coverslipped.

5. DISCUSSION

CA IX is a transmembrane glycoprotein that is overexpressed in many solid tumors.

In the era of *targeted therapy*, several carbonic anhydrase inhibitors are available. Among these agents, some target CA IX. However, they still show some limitations, among which there is the poor specificity, because of high degree of homology among the catalytic sites of the various mammalian CA, with subsequent side effects deriving from inhibition of ubiquitous physiological intracellular CAs, such as CA II.

An alternative strategy to target CA IX may be the design and development of peptide mimetics that are capable to compete for interactions. To design these antagonists it is necessary to characterize the protein network involving CA IX.

Even though scientific literature contains many data about CA IX functions and, more specifically, about its involvement in tumor progression, few studies describe binding partners through which it acts.

Scientific work described in this PhD thesis represents the first and unique study aimed to characterize the interactome of CA IX, until now.

CA IX interactome was characterized in HEK-293 cells, in both normoxia and hypoxia, as CA IX expression is mainly driven by HIF-1.

Its characterization allowed to discover an unexpected protein network of potential interactors, mainly represented by cytosolic and nuclear proteins, such as those involved in nucleocytoplasmic transport and, among others CAND1 and CAND2, regulating protein degradation and gene transcription.

This strongly suggests that CA IX may play additional roles inside tumor cells, besides those already known of pH regulation and facilitation of cell migration.

Among nucleocytoplasmic transport factors, XPO1 has been chosen as the representative member of the whole pathway for validation of interactomic results. As well-known, it drives active transport of proteins and mRNAs involved in ribosomal biogenesis across the NPCs.

As so far CA IX has been described as an enzyme located at the plasma membrane, firstly its subcellular distribution was compared in a panel of four cell lines to investigate its expression pattern in tissues of different embryonic origin. So it has

been observed that CA IX distribution in human colon adenocarcinoma cell line GEO is that “canonical” at the plasma membrane, even if a weak nuclear and perinuclear staining was anyhow detectable. Conversely, a broad subcellular distribution, including nuclear localization, was observed in HEK-293, SH-SY5Y and BJ5T α cells. As the antibody used to visualize CA IX in these cell lines is directed against the extracellular region of CA IX, it follows that is the full length protein to be translocated into the nucleus, similarly to some RTKs undergoing nuclear import.

This intracellular and, especially, nuclear localization of CA IX has been further deepened in HEK-293 cells, where hypoxic treatment seems to stimulate internalization of CA IX and its accumulation in the nucleus and in the nucleoli. Co-localization of CA IX and XPO1 in the nucleoli in hypoxia further confirms biochemical validation through co-precipitation experiments with both strep-tagged and endogenous CA IX.

Occurrence of this interaction in hypoxia rather than in normoxia may derive from increased expression of CA IX under hypoxic conditions or from activation of specific intracellular pathways that modify, through post-translational modifications, these proteins when cells are subjected to hypoxic stress.

In particular, as suggested from pull-down experiments with synthetic peptides, CA IX phosphorylation may stabilize this interaction in hypoxia.

Also interaction of CA IX with TNPO1 has been biochemically validated. As TNPO1 drives transport of proteins in the nucleus, such as transcription factors, co-factors of transcription and mRNA binding proteins, strong interaction between them supports the hypothesis that CA IX may take part to mechanisms that regulate transcription, as shown for EGFR^{232, 233}, ErbB2²³⁴, ErbB4²³⁵.

A hypothetical nuclear function for CA IX was already proposed on the basis of its ability to bind DNA in DNA-cellulose chromatography²⁷.

Moreover bioinformatic analysis highlighted the presence of a stretch of basic amino acids able to bind DNA.

On the basis of CA IX localization in the nucleoli, where it seems to interact with ribosomal proteins, such as RPS5 and with XPO1, an involvement of CA IX in ribosomal biogenesis may be also hypothesized.

CA IX minimal region required for validated interactions with XPO1, TNPO1 and CAND1 has been identified and comprises the intracellular tail and 16 amino acids of

the transmembrane region; it has been shown that all these interactions occur much more when T443 and Y449 are phosphorylated. Within this region putative NES and NLS sequences have been identified. Fusion constructs between reporter protein GFP and these putative sequences were generated to analyze their capability to drive GFP distribution within transfected HEK-293 cells. Results emerged from immunofluorescence analysis on these cells suggest the full functionality of these sequences, that have demonstrated to mediate both import and export processes in and from the nucleus, respectively.

It is known that hypoxia modulates many pathways whose members resulted to be potential interactors of CA IX: nucleocytoplasmic transport²³⁶⁻²³⁸, ribosome biogenesis, translation and protein degradation²³⁹.

CAND1 is a nuclear protein: on one hand it was described as a factor activating basal transcription in vitro, in a dose-dependent manner, through the stimulation of recruitment of TFIIF/RNAPII into a pre-initiation complex; on the other hand it inhibits assembly of SCF E3 ubiquitin ligase complex, involved in the degradation of specific substrates by the proteasome 26S.

Biochemical data, from co-precipitation experiments performed with strep-tagged CA IX, confirmed interaction between CA IX and CAND1.

It is worth to highlight that CAND1 is one of few binding partners interacting with CA IX both in normoxia and hypoxia, even if under hypoxic conditions their binding is more pronounced.

To better investigate and functionally understand interactions between these two proteins, stable pools of clones from HEK-293 cells interfered with CAND1 or CA IX were generated through RNA interference technology.

Preliminary data from HEK-293 clones interfered with CAND1 mRNA expression showed a decrease in CA IX protein in comparison to clones interfered with a non silencing construct, suggesting that CAND1 may be involved in CA IX protein stabilization. This might explain CA IX accumulation in hypoxic conditions in HEK-293 cells transfected with the strep-tagged protein, whose expression in hypoxia is not driven by HIF-1 α stabilization, as CMV promoter lacks HRE element.

In the same way shRNAs interfering with CA IX mRNA expression were transfected in HEK-293 cells to generate stable pools of clones interfered with CA IX but

unfortunately without obtaining clones, probably because of involvement of CA IX in cell survival (data not shown).

That of CA IX is not the unique case of a transmembrane protein that is also found in the nucleus. Many cases are described in scientific literature of transmembrane receptors that enter the nucleus via the transportin-dependent pathway and function as nuclear signal transducers; c-Erb-B2, EGFR, FGFR and CD44 are only some of many known examples²⁴⁰⁻²⁴².

CA IX demonstrated to be a more highly versatile carbonic anhydrase. CA IX role at the plasma membrane as pH regulator and active player in cancer cell migration represents only part of different functions in which CA IX is involved.

6. ACKNOWLEDGEMENTS

... and here I am to the acknowledgments!!!

It 's really difficult to thank all the people who have accompanied me in these 4 years of my PhD program.

For me, being a SEMM student has always been a great pride and a great responsibility; so, first of all, I would like to thank those who allowed me to become one.

Then I would like to thank my supervisor, Prof. N. Zambrano, who has been, and continues to be, my reference model for the deep passion for scientific research and teaching, dedication to work, critical approach to scientific data and results and also for exceptional human qualities. He taught me what it means to become a researcher.

A heartfelt thanks goes to all colleagues and students in the lab: Monica, Pasquale, Stefano, Mariangela Succoio, Antonella, Mariangela Sabatella, Bianca, Emanuele and Luca; together we have formed a really great team and we have shared all gratifications and disappointments coming from the research. Each of them has contributed to my personal and professional growth until now.

Another acknowledgment, that is not enough to enclose all my gratitude, goes to Francesco, without whom my 4 years at the CEINGE and in Naples would not be the same.

Moreover I would like to express my dutiful thanks to Dr. G. Minopoli to have contributed to my training and to my Internal- Co-Supervisor, Prof. L. Del Vecchio, and to my External Co-Supervisor, Prof. F. Maina, that have supported me during my research activity in a critical manner.

Then an overall thanks is for the whole “CEINGE family” that made me feel *at home*, and more specifically for Anna Lucia and for research groups of Prof. Russo, Prof. Iolascon and Prof. Pastore.

Finally I thank my mother, my relatives and my closest friends, that have always supported and encouraged me during these years, even in more difficult moments.

Thanks to all!!!

REFERENCES

1. Supuran, C. T., Carbonic anhydrases: novel therapeutic applications for inhibitors and activators. *Nat Rev Drug Discov* **2008**, 7, (2), 168-81.
2. Scozzafava, A.; et al., Carbonic anhydrase inhibitors and activators and their use in therapy. *Expert. Opin. Ther. Pat* **2006**, 16, 1627-1664.
3. Supuran, C. T.; et al., Carbonic Anhydrase—Its inhibitors and Activators. *CRC, Boca Raton* **2004**, P 1-363.
4. Supuran, C. T.; et al., Carbonic anhydrase inhibitors. *Med Res Rev* **2003**, 23, (2), 146-89.
5. Pastorekova, S.; et al., Carbonic anhydrases: current state of the art, therapeutic applications and future prospects. *J Enzyme Inhib Med Chem* **2004**, 19, (3), 199-229.
6. Nishimori, I.; et al., Carbonic anhydrase inhibitors. The mitochondrial isozyme VB as a new target for sulfonamide and sulfamate inhibitors. *J Med Chem* **2005**, 48, (24), 7860-6.
7. Vullo, D.; et al., Carbonic anhydrase inhibitors. Inhibition of the human cytosolic isozyme VII with aromatic and heterocyclic sulfonamides. *Bioorg Med Chem Lett* **2005**, 15, (4), 971-6.
8. Kohler, K.; et al., Saccharin inhibits carbonic anhydrases: possible explanation for its unpleasant metallic aftertaste. *Angew Chem Int Ed Engl* **2007**, 46, (40), 7697-9.
9. Supuran.; et al., Carbonic anhydrase inhibitors. Part 29. Interaction of isozymes I, II and IV with benzolamide-like derivatives. *Eur. J. Med. Chem* **1998**, 33, 739-752.
10. Supuran, C. T.; et al., Carbonic anhydrase inhibitors: synthesis of sulfonamides incorporating 2,4,6-trisubstituted-pyridinium-ethylcarboxamido moieties possessing membrane-impermeability and in vivo selectivity for the membrane-bound (CA IV) versus the cytosolic (CA I and CA II) isozymes. *J Enzyme Inhib* **2000**, 15, (4), 381-401.
11. Winum, J. Y.; et al., Carbonic anhydrase inhibitors: clash with Ala65 as a means for designing inhibitors with low affinity for the ubiquitous isozyme II, exemplified by the crystal structure of the topiramate sulfamide analogue. *J Med Chem* **2006**, 49, (24), 7024-31.
12. Saczewski, F.; et al., Carbonic anhydrase inhibitors. Inhibition of the cytosolic human isozymes I and II, and the transmembrane, tumor-associated isozymes IX and XII with substituted aromatic sulfonamides activatable in hypoxic tumors. *Bioorg Med Chem Lett* **2006**, 16, (18), 4846-51.
13. De Simone, G.; et al., Carbonic anhydrase inhibitors: Hypoxia-activatable sulfonamides incorporating disulfide bonds that target the tumor-associated isoform IX. *J Med Chem* **2006**, 49, (18), 5544-51.
14. Saari, S.; et al., The most recently discovered carbonic anhydrase, CA XV, is expressed in the thick ascending limb of Henle and in the collecting ducts of mouse kidney. *PLoS One* **2010**, 5, (3), e9624.
15. Pastorekova, S.; et al., Carbonic anhydrase IX (CA IX) as a potential target for cancer therapy. *Cancer Therapy* **2004** Vol 2, 245-262.
16. Kivela, A. J.; et al., Carbonic anhydrases in normal gastrointestinal tract and gastrointestinal tumours. *World J Gastroenterol* **2005**, 11, (2), 155-63.
17. Sethi, K. K.; et al., Carbonic Anhydrase I and II Inhibition with Natural Products: Leucas cephalotes. *Pharmacognosy Communications* **Oct-Dec 2011**, 1 (2), 41-46.
18. Tureci, O.; et al., Human carbonic anhydrase XII: cDNA cloning, expression, and chromosomal localization of a carbonic anhydrase gene that is overexpressed in some renal cell cancers. *Proc Natl Acad Sci U S A* **1998**, 95, (13), 7608-13.
19. Potter, C. et al., Hypoxia inducible carbonic anhydrase IX, marker of tumour hypoxia, survival pathway and therapy target. *Cell Cycle* **2004**, 3, (2), 164-7.
20. Chia, S. K.; et al., Prognostic significance of a novel hypoxia-regulated marker, carbonic anhydrase IX, in invasive breast carcinoma. *J Clin Oncol* **2001**, 19, (16), 3660-8.
21. Hussain, S. A.; et al., Hypoxia-regulated carbonic anhydrase IX expression is associated with poor survival in patients with invasive breast cancer. *Br J Cancer* **2007**, 96, (1), 104-9.
22. Swinson, D. E.; et al., Carbonic anhydrase IX expression, a novel surrogate marker of tumor hypoxia, is associated with a poor prognosis in non-small-cell lung cancer. *J Clin Oncol* **2003**, 21, (3), 473-82.

23. Trastour, C.; et al., HIF-1alpha and CA IX staining in invasive breast carcinomas: prognosis and treatment outcome. *Int J Cancer* **2007**, 120, (7), 1451-8.
24. Potter, C. P.; et al., Diagnostic, prognostic and therapeutic implications of carbonic anhydrases in cancer. *Br J Cancer* **2003**, 89, (1), 2-7.
25. Pastorekova, S.; et al., A novel quasi-viral agent, MaTu, is a two-component system. *Virology* **1992**, 187, (2), 620-6.
26. Zavada, J.; et al., Expression of MaTu-MN protein in human tumor cultures and in clinical specimens. *Int J Cancer* **1993**, 54, (2), 268-74.
27. Pastorek, J.; et al., Cloning and characterization of MN, a human tumor-associated protein with a domain homologous to carbonic anhydrase and a putative helix-loop-helix DNA binding segment. *Oncogene* **1994**, 9, (10), 2877-88.
28. Hewett-Emmett, D.; et al., Functional diversity, conservation, and convergence in the evolution of the alpha-, beta-, and gamma-carbonic anhydrase gene families. *Mol Phylogenet Evol* **1996**, 5, (1), 50-77.
29. Opavsky, R.; et al., Human MN/CA9 gene, a novel member of the carbonic anhydrase family: structure and exon to protein domain relationships. *Genomics* **1996**, 33, (3), 480-7.
30. Nakagawa, Y.; et al., Radiation hybrid mapping of the human MN/CA9 locus to chromosome band 9p12-p13. *Genomics* **1998**, 53, (1), 118-9.
31. Kaluz, S.; et al., Transcriptional regulation of the MN/CA 9 gene coding for the tumor-associated carbonic anhydrase IX. Identification and characterization of a proximal silencer element. *J Biol Chem* **1999**, 274, (46), 32588-95.
32. Wykoff, C. C.; et al., Hypoxia-inducible expression of tumor-associated carbonic anhydrases. *Cancer Res* **2000**, 60, (24), 7075-83.
33. Grabmaier, K.; et al., Strict regulation of CAIX(G250/MN) by HIF-1alpha in clear cell renal cell carcinoma. *Oncogene* **2004**, 23, (33), 5624-31.
34. Kaluz, S.; et al., Expression of the hypoxia marker carbonic anhydrase IX is critically dependent on SP1 activity. Identification of a novel type of hypoxia-responsive enhancer. *Cancer Res* **2003**, 63, (5), 917-22.
35. Kaluzova, M.; et al., Characterization of the MN/CA 9 promoter proximal region: a role for specificity protein (SP) and activator protein 1 (AP1) factors. *Biochem J* **2001**, 359, (Pt 3), 669-77.
36. Ivanov, S.; et al., Expression of hypoxia-inducible cell-surface transmembrane carbonic anhydrases in human cancer. *Am J Pathol* **2001**, 158, (3), 905-19.
37. Kaluz, S.; et al., Proteasomal inhibition attenuates transcriptional activity of hypoxia-inducible factor 1 (HIF-1) via specific effect on the HIF-1alpha C-terminal activation domain. *Mol Cell Biol* **2006**, 26, (15), 5895-907.
38. Wang, G. L.; et al., Hypoxia-inducible factor 1 is a basic-helix-loop-helix-PAS heterodimer regulated by cellular O₂ tension. *Proc Natl Acad Sci U S A* **1995**, 92, (12), 5510-4.
39. Jaakkola, P.; et al., Targeting of HIF-alpha to the von Hippel-Lindau ubiquitylation complex by O₂-regulated prolyl hydroxylation. *Science* **2001**, 292, (5516), 468-72.
40. Maxwell, P. H.; et al., The tumour suppressor protein VHL targets hypoxia-inducible factors for oxygen-dependent proteolysis. *Nature* **1999**, 399, (6733), 271-5.
41. Lando, D.; et al., FIH-1 is an asparaginyl hydroxylase enzyme that regulates the transcriptional activity of hypoxia-inducible factor. *Genes Dev* **2002**, 16, (12), 1466-71.
42. Lando, D.; et al., Asparagine hydroxylation of the HIF transactivation domain a hypoxic switch. *Science* **2002**, 295, (5556), 858-61.
43. Schofield, C. J.; et al., *Nat Rev Mol Cell Biol* **2004**, 5, (5), 343-54.
44. Kaluz, S.; et al., Transcriptional control of the tumor- and hypoxia-marker carbonic anhydrase 9: A one transcription factor (HIF-1) show? *Biochim Biophys Acta* **2009**, 1795, (2), 162-72.
45. Ivanov, S. V.; et al., Down-regulation of transmembrane carbonic anhydrases in renal cell carcinoma cell lines by wild-type von Hippel-Lindau transgenes. *Proc Natl Acad Sci U S A* **1998**, 95, (21), 12596-601.
46. Kaluzova, M.; et al., DNA damage is a prerequisite for p53-mediated proteasomal degradation of HIF-1alpha in hypoxic cells and downregulation of the hypoxia marker carbonic anhydrase IX. *Mol Cell Biol* **2004**, 24, (13), 5757-66.

47. Blagosklonny, M. V.; et al., p53 inhibits hypoxia-inducible factor-stimulated transcription. *J Biol Chem* **1998**, 273, (20), 11995-8.
48. Kopacek, J.; et al., MAPK pathway contributes to density- and hypoxia-induced expression of the tumor-associated carbonic anhydrase IX. *Biochim Biophys Acta* **2005**, 1729, (1), 41-9.
49. Kaluz, S.; et al., Lowered oxygen tension induces expression of the hypoxia marker MN/carbonic anhydrase IX in the absence of hypoxia-inducible factor 1 alpha stabilization: a role for phosphatidylinositol 3'-kinase. *Cancer Res* **2002**, 62, (15), 4469-77.
50. Bardos, J. I.; et al., Hypoxia-inducible factor-1 and oncogenic signalling. *Bioessays* **2004**, 26, (3), 262-9.
51. Dewhirst, M. W.; et al., Cycling hypoxia and free radicals regulate angiogenesis and radiotherapy response. *Nat Rev Cancer* **2008**, 8, (6), 425-37.
52. Barathova, M.; et al., Alternative splicing variant of the hypoxia marker carbonic anhydrase IX expressed independently of hypoxia and tumour phenotype. *Br J Cancer* **2008**, 98, (1), 129-36.
53. Alterio, V.; et al., Crystal structure of the catalytic domain of the tumor-associated human carbonic anhydrase IX. *Proc Natl Acad Sci U S A* **2009**, 106, (38), 16233-8.
54. Hilvo, M.; et al., Biochemical characterization of CA IX, one of the most active carbonic anhydrase isozymes. *J Biol Chem* **2008**, 283, (41), 27799-809.
55. Pastorekova, S.; et al., Cancer-associated carbonic anhydrases and their inhibition. *Curr Pharm Des* **2008**, 14, (7), 685-98.
56. Zavada, J.; et al., Human tumour-associated cell adhesion protein MN/CA IX: identification of M75 epitope and of the region mediating cell adhesion. *Br J Cancer* **2000**, 82, (11), 1808-13.
57. Zavadova, Z.; et al., Carbonic anhydrase IX (CA IX) mediates tumor cell interactions with microenvironment. *Oncol Rep* **2005**, 13, (5), 977-82.
58. Svastova, E.; et al., Carbonic anhydrase IX reduces E-cadherin-mediated adhesion of MDCK cells via interaction with beta-catenin. *Exp Cell Res* **2003**, 290, (2), 332-45.
59. Beavon, I. R., Regulation of E-cadherin: does hypoxia initiate the metastatic cascade? *Mol Pathol* **1999**, 52, (4), 179-88.
60. Innocenti, A.; et al., The proteoglycan region of the tumor-associated carbonic anhydrase isoform IX acts as an intrinsic buffer optimizing CO₂ hydration at acidic pH values characteristic of solid tumors. *Bioorg Med Chem Lett* **2009**, 19, (20), 5825-8.
61. Zavada, J.; et al., Soluble form of carbonic anhydrase IX (CA IX) in the serum and urine of renal carcinoma patients. *Br J Cancer* **2003**, 89, (6), 1067-71.
62. Zatovicova, M.; et al., Ectodomain shedding of the hypoxia-induced carbonic anhydrase IX is a metalloprotease-dependent process regulated by TACE/ADAM17. *Br J Cancer* **2005**, 93, (11), 1267-76.
63. Svastova, E.; et al., Carbonic anhydrase IX interacts with bicarbonate transporters in lamellipodia and increases cell migration via its catalytic domain. *J Biol Chem* **2012**, 287, (5), 3392-402.
64. Hulikova, A.; et al., Intact intracellular tail is critical for proper functioning of the tumor-associated, hypoxia-regulated carbonic anhydrase IX. *FEBS Lett* **2009**, 583, (22), 3563-8.
65. Dorai, T.; et al., The role of carbonic anhydrase IX overexpression in kidney cancer. *Eur J Cancer* **2005**, 41, (18), 2935-47.
66. Buanne, P.; et al., Characterization of Carbonic Anhydrase IX Interactome Reveals Proteins Assisting Its Nuclear Localization in Hypoxic Cells. *J Proteome Res* **2013**, 12, (1), 282-292.
67. Turner, K. J.; et al., The hypoxia-inducible genes VEGF and CA9 are differentially regulated in superficial vs invasive bladder cancer. *Br J Cancer* **2002**, 86, (8), 1276-82.
68. Rafajova, M.; et al., Induction by hypoxia combined with low glucose or low bicarbonate and high posttranslational stability upon reoxygenation contribute to carbonic anhydrase IX expression in cancer cells. *Int J Oncol* **2004**, 24, (4), 995-1004.

69. Vordermark, D.; et al., Characterization of carbonic anhydrase IX (CA IX) as an endogenous marker of chronic hypoxia in live human tumor cells. *Int J Radiat Oncol Biol Phys* **2005**, 61, (4), 1197-207.
70. Jiang, B. H.; et al., Hypoxia-inducible factor 1 levels vary exponentially over a physiologically relevant range of O₂ tension. *Am J Physiol* **1996**, 271, (4 Pt 1), C1172-80.
71. Sobhanifar, S.; et al., Reduced expression of hypoxia-inducible factor-1alpha in perinecrotic regions of solid tumors. *Cancer Res* **2005**, 65, (16), 7259-66.
72. Ord, J. J.; et al., An investigation into the prognostic significance of necrosis and hypoxia in high grade and invasive bladder cancer. *J Urol* **2007**, 178, (2), 677-82.
73. Swietach, P.; et al., Regulation of tumor pH and the role of carbonic anhydrase 9. *Cancer Metastasis Rev* **2007**, 26, (2), 299-310.
74. Hutchison, G. J.; et al., Hypoxia-inducible factor 1alpha expression as an intrinsic marker of hypoxia: correlation with tumor oxygen, pimonidazole measurements, and outcome in locally advanced carcinoma of the cervix. *Clin Cancer Res* **2004**, 10, (24), 8405-12.
75. Sung, F. L.; et al., Genome-wide expression analysis using microarray identified complex signaling pathways modulated by hypoxia in nasopharyngeal carcinoma. *Cancer Lett* **2007**, 253, (1), 74-88.
76. Koukourakis, M. I.; et al., Hypoxia-activated tumor pathways of angiogenesis and pH regulation independent of anemia in head-and-neck cancer. *Int J Radiat Oncol Biol Phys* **2004**, 59, (1), 67-71.
77. Trastour, C.; et al., HIF-1alpha and CA IX staining in invasive breast carcinomas: prognosis and treatment outcome. *Int J Cancer* **2007**, 120, (7), 1451-8.
78. Dorai, T.; et al., Role of carbonic anhydrases in the progression of renal cell carcinoma subtypes: proposal of a unified hypothesis. *Cancer Invest* **2006**, 24, (8), 754-79.
79. Gnarra, J. R.; et al., Mutations of the VHL tumour suppressor gene in renal carcinoma. *Nat Genet* **1994**, 7, (1), 85-90.
80. Kaelin, W. G., Jr., Molecular basis of the VHL hereditary cancer syndrome. *Nat Rev Cancer* **2002**, 2, (9), 673-82.
81. Wiesener, M. S.; et al., activation of hypoxia-inducible genes related to overexpression of hypoxia-inducible factor-1alpha in clear cell renal carcinomas. *Cancer Res* **2001**, 61, (13), 5215-22.
82. Bui, M. H.; et al., Carbonic anhydrase IX is an independent predictor of survival in advanced renal clear cell carcinoma: implications for prognosis and therapy. *Clin Cancer Res* **2003**, 9, (2), 802-11.
83. Lancaster, J. A.; et al., Carbonic anhydrase (CA IX) expression, a potential new intrinsic marker of hypoxia: correlations with tumor oxygen measurements and prognosis in locally advanced carcinoma of the cervix. *Cancer Res* **2001**, 61, (17), 6394-9.
84. Hoskin, P. J.; et al., GLUT1 and CAIX as intrinsic markers of hypoxia in bladder cancer: relationship with vascularity and proliferation as predictors of outcome of ARCON. *Br J Cancer* **2003**, 89, (7), 1290-7.
85. Diaz-Gonzalez, J. A.; et al., Targeting hypoxia and angiogenesis through HIF-1alpha inhibition. *Cancer Biol Ther* **2005**, 4, (10), 1055-62.
86. Neri, D.; et al., Interfering with pH regulation in tumours as a therapeutic strategy. *Nat Rev Drug Discov* **2010**, 10, (10), 767-77.
87. Gatenby, R. A.; Gillies, R. J., Why do cancers have high aerobic glycolysis? *Nat Rev Cancer* **2004**, 4, (11), 891-9.
88. Brahimi-Horn, M. C.; et al., Hypoxia and energetic tumour metabolism. *Curr Opin Genet Dev* **2011**, 21, (1), 67-72.
89. Parks, S. K.; et al., pH control mechanisms of tumor survival and growth. *J Cell Physiol* **2011**, 226, (2), 299-308.
90. Svastova, E.; et al., activates the capacity of tumor-associated carbonic anhydrase IX to acidify extracellular pH. *FEBS Lett* **2004**, 577, (3), 439-45.
91. Chiche, J.; et al., Hypoxia-inducible carbonic anhydrase IX and XII promote tumor cell growth by counteracting acidosis through the regulation of the intracellular pH. *Cancer Res* **2009**, 69, (1), 358-68.

92. Thiry, A.; et al., Targeting tumor-associated carbonic anhydrase IX in cancer therapy. *Trends Pharmacol Sci* **2006**, 27, (11), 566-73.
93. Cecchi, A.; et al., Carbonic anhydrase inhibitors. Design of fluorescent sulfonamides as probes of tumor-associated carbonic anhydrase IX that inhibit isozyme IX-mediated acidification of hypoxic tumors. *J Med Chem* **2005**, 48, (15), 4834-41.
94. Dubois, L.; et al., Imaging the hypoxia surrogate marker CA IX requires expression and catalytic activity for binding fluorescent sulfonamide inhibitors. *Radiother Oncol* **2007**, 83, (3), 367-73.
95. Brahimi-Horn, M. C.; et al., Hypoxia in cancer cell metabolism and pH regulation. *Essays Biochem* **2007**, 43, 165-78.
96. Ebbesen, P.; et al., Taking advantage of tumor cell adaptations to hypoxia for developing new tumor markers and treatment strategies. *J Enzyme Inhib Med Chem* **2009**, 24 Suppl 1, 1-39.
97. Swietach, P.; et al., Tumor-associated carbonic anhydrase 9 spatially coordinates intracellular pH in three-dimensional multicellular growths. *J Biol Chem* **2008**, 283, (29), 20473-83.
98. Swietach, P.; et al., The role of carbonic anhydrase 9 in regulating extracellular and intracellular pH in three-dimensional tumor cell growths. *J Biol Chem* **2009**, 284, (30), 20299-310
99. Sauvant, C.; et al., Acidosis induces multi-drug resistance in rat prostate cancer cells (AT1) in vitro and in vivo by increasing the activity of the p-glycoprotein via activation of p38. *Int J Cancer* **2008**, 123, (11), 2532-42.
100. Gerweck, L. E.; et al., Cellular pH gradient in tumor versus normal tissue: potential exploitation for the treatment of cancer. *Cancer Res* **1996**, 56, (6), 1194-8.
101. Raghunand, N.; et al., Enhancement of chemotherapy by manipulation of tumour pH. *Br J Cancer* **1999**, 80, (7), 1005-11.
102. Raghunand, N.; et al., pH and chemotherapy. *Novartis Foundation Symposium* **2001**, 240, 199-211.
103. Zatovicova, M.; et al., Carbonic anhydrase IX as an anticancer therapy target: preclinical evaluation of internalizing monoclonal antibody directed to catalytic domain. *Curr Pharm Des* **2010**, 16, (29), 3255-63.
104. Scozzafava, A.; et al., Carbonic anhydrase inhibitors: synthesis of membrane-impermeant low molecular weight sulfonamides possessing in vivo selectivity for the membrane-bound versus cytosolic isozymes. *J Med Chem* **2000**, 43, (2), 292-300.
105. Cianchi, F.; et al., Selective inhibition of carbonic anhydrase IX decreases cell proliferation and induces ceramide-mediated apoptosis in human cancer cells. *J Pharmacol Exp Ther* **2010**, 334, (3), 710-9.
106. Bao, B.; et al., In vivo imaging and quantification of carbonic anhydrase IX expression as an endogenous biomarker of tumor hypoxia. *PLoS One* **2012**, 7, (11), e50860.
107. Andrade, M. A.; et al., Protein repeats: structures, functions, and evolution. *J Struct Biol* **2001**, 134, (2-3), 117-31.
108. Marcotte, E. M.; et al., A census of protein repeats. *J Mol Biol* **1999**, 293, (1), 151-60.
109. Groves, M. R.; Barford, D., Topological characteristics of helical repeat proteins. *Curr Opin Struct Biol* **1999**, 9, (3), 383-9.
110. Kobe, B.; et al., When protein folding is simplified to protein coiling: the continuum of solenoid protein structures. *Trends Biochem Sci* **2000**, 25, (10), 509-15.
111. Andrade, M. A.; et al., Comparison of ARM and HEAT protein repeats. *J Mol Biol* **2001**, 309, (1), 1-18.
112. Riggleman, B.; et al., Molecular analysis of the armadillo locus: uniformly distributed transcripts and a protein with novel internal repeats are associated with a Drosophila segment polarity gene. *Genes Dev* **1989**, 3, (1), 96-113.
113. Franke, W. W.; et al., cloning and amino acid sequence of human plakoglobin, the common junctional plaque protein. *Proc Natl Acad Sci U S A* **1989**, 86, (11), 4027-31.
114. Peifer, M.; et al., A repeating amino acid motif shared by proteins with diverse cellular roles. *Cell* **1994**, 76, (5), 789-91.
115. Gorlich, D.; et al., Isolation of a protein that is essential for the first step of nuclear protein import. *Cell* **1994**, 79, (5), 767-78.

116. Andrade, M. A.; et al., HEAT repeats in the Huntington's disease protein. *Nat Genet* **1995**, 11, (2), 115-6.
117. Andrade, M. A.; et al., Homology-based method for identification of protein repeats using statistical significance estimates. *J Mol Biol* **2000**, 298, (3), 521-37.
118. Neuwald, A. F.; et al., HEAT repeats associated with condensins, cohesins, and other complexes involved in chromosome-related functions. *Genome Res* **2000**, 10, (10), 1445-52.
119. Malik, H. S.; et al., Evolutionary specialization of the nuclear targeting apparatus. *Proc Natl Acad Sci U S A* **1997**, 94, (25), 13738-42.
120. Cingolani, G.; et al., Structure of importin-beta bound to the IBB domain of importin-alpha. *Nature* **1999**, 399, (6733), 221-9.
121. Kobe, B.; et al., Turn up the HEAT. *Structure* **1999**, 7, (5), R91-7.
122. Rout, M. P.; et al., Pore relations: nuclear pore complexes and nucleocytoplasmic exchange. *Essays Biochem* **2000**, 36, 75-88.
123. Cronshaw, J. M.; et al., Proteomic analysis of the mammalian nuclear pore complex. *J Cell Biol* **2002**, 158, (5), 915-27.
124. Conti, E.; et al., Karyopherin flexibility in nucleocytoplasmic transport. *Curr Opin Struct Biol* **2006**, 16, (2), 237-44.
125. Cook, A.; et al., Structural biology of nucleocytoplasmic transport. *Annu Rev Biochem* **2007**, 76, 647-71.
126. Marg, A.; et al., Nucleocytoplasmic shuttling by nucleoporins Nup153 and Nup214 and CRM1-dependent nuclear export control the subcellular distribution of latent Stat1. *J Cell Biol* **2004**, 165, (6), 823-33.
127. Stenina, O. I.; et al., Thrombin activates a Y box-binding protein (DNA-binding protein B) in endothelial cells. *J Clin Invest* **2000**, 106, (4), 579-87.
128. Gorlich, D.; et al., Two different subunits of importin cooperate to recognize nuclear localization signals and bind them to the nuclear envelope. *Curr Biol* **1995**, 5, (4), 383-92.
129. Imamoto, N.; et al., The nuclear pore-targeting complex binds to nuclear pores after association with a karyophile. *FEBS Lett* **1995**, 368, (3), 415-9.
130. Chi, N. C.; et al., Sequence and characterization of cytoplasmic nuclear protein import factor p97. *J Cell Biol* **1995**, 130, (2), 265-74.
131. Radu, A.; et al., Identification of a protein complex that is required for nuclear protein import and mediates docking of import substrate to distinct nucleoporins. *Proc Natl Acad Sci U S A* **1995**, 92, (5), 1769-73.
132. Sorokin, A. V.; et al., Nucleocytoplasmic transport of proteins. *Biochemistry (Mosc)* **2007**, 72, (13), 1439-57.
133. Kudo, N.; et al., Leptomycin B inactivates CRM1/exportin 1 by covalent modification at a cysteine residue in the central conserved region. *Proc Natl Acad Sci U S A* **1999**, 96, (16), 9112-7.
134. Wolff, B.; et al., Leptomycin B is an inhibitor of nuclear export: inhibition of nucleocytoplasmic translocation of the human immunodeficiency virus type 1 (HIV-1) Rev protein and Rev-dependent mRNA. *Chem Biol* **1997**, 4, (2), 139-47.
135. Lei, E. P.; et al., Protein and RNA export from the nucleus. *Dev Cell* **2002**, 2, (3), 261-72.
136. Kim, V. N., MicroRNA precursors in motion: exportin-5 mediates their nuclear export. *Trends Cell Biol* **2004**, 14, (4), 156-9.
137. Zeng, Y.; et al., Structural requirements for pre-microRNA binding and nuclear export by Exportin 5. *Nucleic Acids Res* **2004**, 32, (16), 4776-85.
138. Weis, K., Regulating access to the genome: nucleocytoplasmic transport throughout the cell cycle. *Cell* **2003**, 112, (4), 441-51.
139. Dasso, M., The Ran GTPase: theme and variations. *Curr Biol* **2002**, 12, (14), R502-8.
140. Bischoff, F. R.; et al., RanBP1 is crucial for the release of RanGTP from importin beta-related nuclear transport factors. *FEBS Lett* **1997**, 419, (2-3), 249-54.
141. Bischoff, F. R.; et al., Co-activation of RanGTPase and inhibition of GTP dissociation by Ran-GTP binding protein RanBP1. *EMBO J* **1995**, 14, (4), 705-15.

142. Coutavas, E.; et al., Characterization of proteins that interact with the cell-cycle regulatory protein Ran/TC4. *Nature* **1993**, 366, (6455), 585-7.
143. Delphin, C.; et al., RanGTP targets p97 to RanBP2, a filamentous protein localized at the cytoplasmic periphery of the nuclear pore complex. *Mol Biol Cell* **1997**, 8, (12), 2379-90.
144. Mahajan, R.; et al., A small ubiquitin-related polypeptide involved in targeting RanGAP1 to nuclear pore complex protein RanBP2. *Cell* **1997**, 88, (1), 97-107.
145. Matunis, M. J.; et al., A novel ubiquitin-like modification modulates the partitioning of the Ran-GTPase-activating protein RanGAP1 between the cytosol and the nuclear pore complex. *J Cell Biol* **1996**, 135, (6 Pt 1), 1457-70.
146. Ribbeck, K.; et al., NTF2 mediates nuclear import of Ran. *EMBO J* **1998**, 17, (22), 6587-98.
147. Smith, A.; et al., Nuclear import of Ran is mediated by the transport factor NTF2. *Curr Biol* **1998**, 8, (25), 1403-6.
148. Gorlich, D.; et al., Identification of different roles for RanGDP and RanGTP in nuclear protein import. *EMBO J* **1996**, 15, (20), 5584-94.
149. Moore, M. S.; et al., Purification of a Ran-interacting protein that is required for protein import into the nucleus. *Proc Natl Acad Sci U S A* **1994**, 91, (21), 10212-6.
150. Nehrbass, U.; et al., Role of the nuclear transport factor p10 in nuclear import. *Science* **1996**, 272, (5258), 120-2.
151. Weis, K.; et al., Characterization of the nuclear protein import mechanism using Ran mutants with altered nucleotide binding specificities. *EMBO J* **1996**, 15, (24), 7120-8.
152. Schlenstedt, G.; et al., The GTP-bound form of the yeast Ran/TC4 homologue blocks nuclear protein import and appearance of poly(A)+ RNA in the cytoplasm. *Proc Natl Acad Sci U S A* **1995**, 92, (1), 225-9.
153. Richards, S. A.; et al., Requirement of guanosine triphosphate-bound ran for signal-mediated nuclear protein export. *Science* **1997**, 276, (5320), 1842-4.
154. Paschal, B. M.; et al., Nucleotide-specific interaction of Ran/TC4 with nuclear transport factors NTF2 and p97. *Proc Natl Acad Sci U S A* **1996**, 93, (15), 7679-83.
155. Nemergut, M. E.; et al., Chromatin docking and exchange activity enhancement of RCC1 by histones H2A and H2B. *Science* **2001**, 292, (5521), 1540-3.
156. Nemergut, M. E.; et al., Ran-binding protein 3 links Crm1 to the Ran guanine nucleotide exchange factor. *J Biol Chem* **2002**, 277, (20), 17385-8.
157. Hershko, A.; et al., The ubiquitin system. *Annu Rev Biochem* **1998**, 67, 425-79.
158. Hochstrasser, M., Ubiquitin-dependent protein degradation. *Annu Rev Genet* **1996**, 30, 405-39.
159. Chau, V.; et al., A multiubiquitin chain is confined to specific lysine in a targeted short-lived protein. *Science* **1989**, 243, (4898), 1576-83.
160. Hershko, A.; et al., The ubiquitin system for protein degradation. *Annu Rev Biochem* **1992**, 61, 761-807.
161. Ciechanover, A., The ubiquitin-proteasome proteolytic pathway. *Cell* **1994**, 79, (1), 13-21.
162. Liu, F.; et al., Multitasking with ubiquitin through multivalent interactions. *Trends Biochem Sci* **2010**, 35, (6), 352-60.
163. Newton, K.; et al., Ubiquitin chain editing revealed by polyubiquitin linkage-specific antibodies. *Cell* **2008**, 134, (4), 668-78.
164. Hofmann, R. M.; et al., Noncanonical MMS2-encoded ubiquitin-conjugating enzyme functions in assembly of novel polyubiquitin chains for DNA repair. *Cell* **1999**, 96, (5), 645-53.
165. Deng, L.; et al., Activation of the I κ B kinase complex by TRAF6 requires a dimeric ubiquitin-conjugating enzyme complex and a unique polyubiquitin chain. *Cell* **2000**, 103, (2), 351-61.
166. Seet, B. T.; et al., Reading protein modifications with interaction domains. *Nat Rev Mol Cell Biol* **2006**, 7, (7), 473-83.
167. Thrower, J. S.; et al., Recognition of the polyubiquitin proteolytic signal. *EMBO J* **2000**, 19, (1), 94-102.

168. van Nocker, S.; et al., The multiubiquitin-chain-binding protein Mub1 is a component of the 26S proteasome in *Saccharomyces cerevisiae* and plays a nonessential, substrate-specific role in protein turnover. *Mol Cell Biol* **1996**, 16, (11), 6020-8.
169. Husnjak, K.; et al., Proteasome subunit Rpn13 is a novel ubiquitin receptor. *Nature* **2008**, 453, (7194), 481-8.
170. Schreiner, P.; et al., Ubiquitin docking at the proteasome through a novel pleckstrin-homology domain interaction. *Nature* **2008**, 453, 548-552.
171. Saeki, Y.; et al., Identification of ubiquitin-like protein-binding subunits of the 26S proteasome. *Biochem Biophys Res Commun* **2002**, 296, (4), 813-9.
172. Verma, R.; et al., Multiubiquitin chain receptors define a layer of substrate selectivity in the ubiquitin-proteasome system. *Cell* **2004**, 118, (1), 99-110.
173. Funakoshi, M.; et al., Budding yeast Dsk2p is a polyubiquitin-binding protein that can interact with the proteasome. *Proc Natl Acad Sci U S A* **2002**, 99, (2), 745-50.
174. Kaplun, L.; et al., The DNA damage-inducible Ubl-UbA protein Ddi1 participates in Mec1-mediated degradation of Ho endonuclease. *Mol Cell Biol* **2005**, 25, (13), 5355-62.
175. Hamazaki, J.; et al., A novel proteasome interacting protein recruits the deubiquitinating enzyme UCH37 to 26S proteasomes. *EMBO J* **2006**, 25, (19), 4524-36.
176. Yao, T.; et al., Proteasome recruitment and activation of the Uch37 deubiquitinating enzyme by Adrm1. *Nat Cell Biol* **2006**, 8, (9), 994-1002.
177. Qiu, X. B.; et al., hRpn13/ADRM1/GP110 is a novel proteasome subunit that binds the deubiquitinating enzyme, UCH37. *EMBO J* **2006**, 25, (24), 5742-53.
178. Liu, F.; et al., Multitasking with ubiquitin through multivalent interactions. *Trends Biochem Sci* **2010**, 35, (6), 352-60.
179. Scheffner, M.; et al., Protein ubiquitination involving an E1-E2-E3 enzyme ubiquitin thioester cascade. *Nature* **1995**, 373, (6509), 81-3.
180. Deshaies, R. J., SCF and Cullin/Ring H2-based ubiquitin ligases. *Annu Rev Cell Dev Biol* **1999**, 15, 435-67.
181. Tyers, M.; et al., Proteolysis and the cell cycle: with this RING I do thee destroy. *Curr Opin Genet Dev* **2000**, 10, (1), 54-64.
182. Page, A. M.; et al., The anaphase-promoting complex: new subunits and regulators. *Annu Rev Biochem* **1999**, 68, 583-609.
183. Joazeiro, C. A.; et al., RING finger proteins: mediators of ubiquitin ligase activity. *Cell* **2000**, 102, (5), 549-52.
184. Carrano, A. C.; et al., SKP2 is required for ubiquitin-mediated degradation of the CDK inhibitor p27. *Nat Cell Biol* **1999**, 1, (4), 193-9.
185. Sutterluty, H.; et al., p45SKP2 promotes p27Kip1 degradation and induces S phase in quiescent cells. *Nat Cell Biol* **1999**, 1, (4), 207-14.
186. Koepf, D. M.; et al., Phosphorylation-dependent ubiquitination of cyclin E by the SCFFbw7 ubiquitin ligase. *Science* **2001**, 294, (5540), 173-7.
187. Moberg, K. H.; et al., Archipelago regulates Cyclin E levels in *Drosophila* and is mutated in human cancer cell lines. *Nature* **2001**, 413, (6853), 311-6.
188. Strohmaier, H.; et al., Human F-box protein hCdc4 targets cyclin E for proteolysis and is mutated in a breast cancer cell line. *Nature* **2001**, 413, (6853), 316-22.
189. Fuchs, S. Y.; et al., HOS, a human homolog of Slimb, forms an SCF complex with Skp1 and Cullin1 and targets the phosphorylation-dependent degradation of I κ B and beta-catenin. *Oncogene* **1999**, 18, (12), 2039-46.
190. Hart, M.; et al., The F-box protein beta-TrCP associates with phosphorylated beta-catenin and regulates its activity in the cell. *Curr Biol* **1999**, 9, (4), 207-10.
191. Latres, E.; et al., The human F box protein beta-Trcp associates with the Cul1/Skp1 complex and regulates the stability of beta-catenin. *Oncogene* **1999**, 18, (4), 849-54.
192. Yaron, A.; et al., Identification of the receptor component of the I κ B α -ubiquitin ligase. *Nature* **1998**, 396, (6711), 590-4.
193. Verma, R.; et al., Phosphorylation of Sic1p by G1 Cdk required for its degradation and entry into S phase. *Science* **1997**, 278, (5337), 455-60.

194. Lanker, S.; et al., Rapid degradation of the G1 cyclin Cln2 induced by CDK-dependent phosphorylation. *Science* **1996**, 271, (5255), 1597-601.
195. Clurman, B. E.; et al., Turnover of cyclin E by the ubiquitin-proteasome pathway is regulated by cdk2 binding and cyclin phosphorylation. *Genes Dev* **1996**, 10, (16), 1979-90.
196. Won, K. A.; et al., Activation of cyclin E/CDK2 is coupled to site-specific autophosphorylation and ubiquitin-dependent degradation of cyclin E. *EMBO J* **1996**, 15, (16), 4182-93.
197. Sheaff, R. J.; et al., Cyclin E-CDK2 is a regulator of p27Kip1. *Genes Dev* **1997**, 11, (11), 1464-78.
198. Yoshida, Y.; et al., E3 ubiquitin ligase that recognizes sugar chains. *Nature* **2002**, 418, (6896), 438-42.
199. Kamura, T.; et al., Rbx1, a component of the VHL tumor suppressor complex and SCF ubiquitin ligase. *Science* **1999**, 284, (5414), 657-61.
200. Skowrya, D.; et al., Reconstitution of G1 cyclin ubiquitination with complexes containing SCFGrr1 and Rbx1. *Science* **1999**, 284, (5414), 662-5.
201. Ohta, T.; et al., ROC1, a homolog of APC11, represents a family of cullin partners with an associated ubiquitin ligase activity. *Mol Cell* **1999**, 3, (4), 535-41.
202. Tan, P.; et al., Recruitment of a ROC1-CUL1 ubiquitin ligase by Skp1 and HOS to catalyze the ubiquitination of I kappa B alpha. *Mol Cell* **1999**, 3, (4), 527-33.
203. Seol, J. H.; et al., Cdc53/cullin and the essential Hrt1 RING-H2 subunit of SCF define a ubiquitin ligase module that activates the E2 enzyme Cdc34. *Genes Dev* **1999**, 13, (12), 1614-26.
204. Skowrya, D.; et al., F-box proteins are receptors that recruit phosphorylated substrates to the SCF ubiquitin-ligase complex. *Cell* **1997**, 91, (2), 209-19.
205. Feldman, R. M.; et al., A complex of Cdc4p, Skp1p, and Cdc53p/cullin catalyzes ubiquitination of the phosphorylated CDK inhibitor Sic1p. *Cell* **1997**, 91, (2), 221-30.
206. Wada, H.; et al., Identification of NEDD8-conjugation site in human cullin-2. *Biochem Biophys Res Commun* **1999**, 257, (1), 100-5.
207. Zheng, N.; et al., Structure of the Cul1-Rbx1-Skp1-F boxSkp2 SCF ubiquitin ligase complex. *Nature* **2002**, 416, (6882), 703-9.
208. Furukawa, M.; et al., The CUL1 C-terminal sequence and ROC1 are required for efficient nuclear accumulation, NEDD8 modification, and ubiquitin ligase activity of CUL1. *Mol Cell Biol* **2000**, 20, (21), 8185-97.
209. Gray, W. M.; et al., Role of the Arabidopsis RING-H2 protein RBX1 in RUB modification and SCF function. *Plant Cell* **2002**, 14, (9), 2137-44.
210. Kamura, T.; et al., The Rbx1 subunit of SCF and VHL E3 ubiquitin ligase activates Rub1 modification of cullins Cdc53 and Cul2. *Genes Dev* **1999**, 13, (22), 2928-33.
211. Liakopoulos, D.; et al., A novel protein modification pathway related to the ubiquitin system. *EMBO J* **1998**, 17, (8), 2208-14.
212. Osaka, F.; et al., A new NEDD8-ligating system for cullin-4A. *Genes Dev* **1998**, 12, (15), 2263-8.
213. Read, M. A.; et al., Nedd8 modification of cul-1 activates SCF(beta(TrCP))-dependent ubiquitination of I kappa B alpha. *Mol Cell Biol* **2000**, 20, (7), 2326-33.
214. Podust, V. N.; et al., A Nedd8 conjugation pathway is essential for proteolytic targeting of p27Kip1 by ubiquitination. *Proc Natl Acad Sci U S A* **2000**, 97, (9), 4579-84.
215. Cope, G. A.; et al., COP9 signalosome: a multifunctional regulator of SCF and other cullin-based ubiquitin ligases. *Cell* **2003**, 114, (6), 663-71.
216. Cope, G. A.; et al., Role of predicted metalloprotease motif of Jab1/Csn5 in cleavage of Nedd8 from Cul1. *Science* **2002**, 298, (5593), 608-11.
217. Zhou, C.; et al., Fission yeast COP9/signalosome suppresses cullin activity through recruitment of the deubiquitylating enzyme Ubp12p. *Mol Cell* **2003**, 11, (4), 927-38.
218. Bornstein, G.; et al., Regulation of neddylation and deneddylation of cullin1 in SCFSkp2 ubiquitin ligase by F-box protein and substrate. *Proc Natl Acad Sci U S A* **2006**, 103, (31), 11515-20.

219. Yogosawa, S.; et al., Molecular cloning of a novel 120-kDa TBP-interacting protein. *Biochem Biophys Res Commun* **1996**, 229, (2), 612-7.
220. Makino, Y.; et al., TATA-Binding protein-interacting protein 120, TIP120, stimulates three classes of eukaryotic transcription via a unique mechanism. *Mol Cell Biol* **1999**, 19, (12), 7951-60.
221. Kayukawa, K.; et al., TBP-interacting protein TIP120A is a new global transcription activator with bipartite functional domains. *Genes Cells* **2001**, 6, (2), 165-74.
222. Yogosawa, S.; et al., Induced expression, localization, and chromosome mapping of a gene for the TBP-interacting protein 120A. *Biochem Biophys Res Commun* **1999**, 266, (1), 123-8.
223. Goldenberg, S. J.; et al., Structure of the Cand1-Cul1-Roc1 complex reveals regulatory mechanisms for the assembly of the multisubunit cullin-dependent ubiquitin ligases. *Cell* **2004**, 119, (4), 517-28.
224. Zheng, G.; et al., Identification of carbonic anhydrase 9 as a contributor to pingyangmycin-induced drug resistance in human tongue cancer cells. *FEBS J* **2010**, 277, (21), 4506-18.
225. Caratu, G.; et al., Identification of the ligands of protein interaction domains through a functional approach. *Mol Cell Proteomics* **2007**, 6, (2), 333-45.
226. Szklarczyk, D.; et al., The STRING database in 2011: functional interaction networks of proteins, globally integrated and scored. *Nucleic Acids Res* **2011**, 39, (Database issue), D561-8
227. Huang da, W.; et al., Systematic and integrative analysis of large gene lists using DAVID bioinformatics resources. *Nat. Protoc* **2009**, 4 (1), 44-57.
228. Huang da, W.; et al., Bioinformatics enrichment tools: paths toward the comprehensive functional analysis of large gene lists. *Nucleic Acids Res* **2009**, 37 (1), 1-13.
229. Nguyen Ba, A. N.; et al., NLStradamus: a simple Hidden Markov Model for nuclear localization signal prediction. *BMC Bioinformatics* **2009** Jun 29;10(1):202.
230. Zat'ovicova, M.; et al., Monoclonal antibodies generated in carbonic anhydrase IX-deficient mice recognize different domains of tumour-associated hypoxia-induced carbonic anhydrase IX. *J Immunol Methods* **2003**, 282, (1-2), 117-34.
231. Fields, G. B.; et al., Solid phase peptide synthesis utilizing 9-fluorenylmethoxycarbonyl amino acids. *Int J Pept Protein Res* **1990**, 35, (3), 161-214.
232. Lin, S. Y.; et al., Nuclear localization of EGF receptor and its potential new role as a transcription factor. *Nat Cell Biol* **2001**, 3, (9), 802-8.
233. Lo, H. W.; et al., Nuclear interaction of EGFR and STAT3 in the activation of the iNOS/NO pathway. *Cancer Cell* **2005**, 7, (6), 575-89.
234. Wang, S. C.; et al., Binding at and transactivation of the COX-2 promoter by nuclear tyrosine kinase receptor ErbB-2. *Cancer Cell* **2004**, 6, (3), 251-61.
235. Ni, C. Y.; et al., gamma -Secretase cleavage and nuclear localization of ErbB-4 receptor tyrosine kinase. *Science* **2001**, 294, (5549), 2179-81.
236. Groulx, I.; et al., Oxygen-dependent ubiquitination and degradation of hypoxia-inducible factor requires nuclear-cytoplasmic trafficking of the von Hippel-Lindau tumor suppressor protein. *Mol Cell Biol* **2002**, 22, (15), 5319-36.
237. Steinhoff, A.; et al., Cellular oxygen sensing: Importins and exportins are mediators of intracellular localisation of prolyl-4-hydroxylases PHD1 and PHD2. *Biochem Biophys Res Commun* **2009**, 387, (4), 705-11.
238. Mylonis, I.; et al., Identification of MAPK phosphorylation sites and their role in the localization and activity of hypoxia-inducible factor-1alpha. *J Biol Chem* **2006**, 281, (44), 33095-106.
239. Koritzinsky, M.; et al., Hypoxia and regulation of messenger RNA translation. *Methods Enzymol* **2007**, 435, 247-73.
240. Giri, D. K.; et al., Endosomal transport of ErbB-2: mechanism for nuclear entry of the cell surface receptor. *Mol Cell Biol* **2005**, 25, (24), 11005-18.
241. Bryant, D. M.; et al., Nuclear translocation of cell-surface receptors: lessons from fibroblast growth factor. *Traffic* **2005**, 6, (10), 947-54.
242. Janiszewska, M.; et al., Transportin regulates nuclear import of CD44. *J Biol Chem* **2010**, 285, (40), 30548-57.